Dimethylsulfide (DMS) production in polar oceans may be insensitive to ocean acidification: a meta-analysis of 18 microcosm experiments from temperate to polar waters.

Frances E. Hopkins[1], Philip D. Nightingale[1], John A. Stephens[1], C. Mark Moore[2], Sophie Richier[2], Gemma L. Cripps[2], Stephen D. Archer[3]

[1] {Plymouth Marine Laboratory, Plymouth, U.K.}

[2] {Ocean and Earth Science, National Oceanography Centre, University of Southampton, Southampton, U.K.}

[3] {Bigelow Laboratory for Ocean Sciences, Maine, U.S.A.}

Correspondence to: Frances E. Hopkins (fhop@pml.ac.uk)

Abstract

Emissions of dimethylsulfide (DMS) from the polar oceans play a key role in atmospheric processes and climate. Therefore, it is important to increase our understanding of how DMS production in these regions may respond to climate change. The polar oceans are particularly vulnerable to ocean acidification (OA). However, our understanding of the polar DMS response is limited to two studies conducted in Arctic waters, where in both cases DMS concentrations decreased with increasing acidity. Here, we report on our findings from seven summertime shipboard microcosm experiments undertaken in a variety of locations in the Arctic Ocean and Southern Ocean. These experiments reveal no significant effects of short term OA on the net production of DMS by planktonic communities. This is in contrast to similar experiments from temperate NW European shelf waters where surface ocean communities responded to OA with significant increases in dissolved DMS concentrations. A meta-analysis of the findings from both temperate and polar waters (n = 18 experiments) reveals clear regional differences in the DMS response to OA. Based on our findings, we hypothesise that the differences in DMS response between temperate and polar waters reflect the natural variability in carbonate chemistry to which the respective communities of each region may already be adapted. This implies that future temperate oceans could be more sensitive to OA resulting in a change in DMS emissions to the atmosphere, whilst perhaps surprisingly DMS emissions from the polar oceans may remain relatively unchanged. By

demonstrating that DMS emissions from geographically distinct regions may vary in their response to OA, our results may facilitate a better understanding of Earth's future climate. Our study suggests that the way in which processes that generate DMS respond to OA may be regionally distinct and this should be taken into account in predicting future DMS emissions and their influence on Earth's climate.

1 Introduction

The trace gas dimethylsulfide (DMS) is a key ingredient in a cocktail of gases that exchange between the ocean and atmosphere. Dissolved DMS is produced via the enzymatic breakdown of dimethylsulfoniopropionate (DMSP), a secondary algal metabolite implicated in a number of cellular roles, including the regulation of carbon and sulfur metabolism via an overflow mechanism (Stefels, 2000) and protection against oxidative stress (Sunda et al., 2002). Oceanic DMS emissions amount to 17 - 34 Tg S y^{-1}, representing 80 - 90% of all marine biogenic S emissions, and up to 50% of global biogenic emissions (Lana et al., 2011). DMS and its oxidation products play vital roles in atmospheric chemistry and climate processes. These processes include aerosol formation pathways that influence the concentration of cloud condensation nuclei (CCN) with implications for Earth's albedo and climate (Charlson et al., 1987; Korhonen et al., 2008a), and the atmospheric oxidation pathways of other key climate gases, including isoprene, ammonia and organohalogens (Chen and Jang, 2012; von Glasow and Crutzen, 2004; Johnson and Bell, 2008). Thus, our ability to predict the climate into the future requires an understanding of how marine DMS production may respond to global change (Carpenter et al., 2012; Woodhouse et al., 2013).

The biologically-rich seas surrounding the Arctic pack ice are a strong source of DMS to the Arctic atmosphere (Levasseur, 2013). A seasonal cycle in CCN numbers can be related to seasonality in the Arctic DMS flux (Chang et al., 2011). Indeed, observations confirm that DMS oxidation products promote the growth of particles to produce aerosols that may influence cloud processes and atmospheric albedo (Bigg and Leck, 2001; Rempillo et al., 2011; Korhonen et al., 2008b; Chang et al., 2011). Arctic new particle formation events and peaks in aerosol optical depth (AOD) occur during summertime clean air periods (when levels of anthropogenic black carbon diminish), and have been linked to chlorophyll *a* maxima in surface waters and the presence of aerosols formed from DMS oxidation products such as methanesulfonate (MSA). The atmospheric oxidation products of DMS - SO_2 and H_2SO_4 - contribute to both the growth of existing particles and new particle formation (NPF)

in the Arctic atmosphere (Leaitch et al., 2013; Gabric et al., 2014; Sharma et al., 2012). Thus, the ongoing and projected rapid loss of seasonal Arctic sea ice may influence the Arctic radiation budget via changes to both the DMS flux and the associated formation and growth of cloud-influencing particles (Sharma et al., 2012).

During its short but highly productive summer season, the Southern Ocean is a hotspot of DMS flux to the atmosphere, influenced by the prevalence of intense blooms of DMSP-rich *Phaeocystis antarctica* (Schoemann et al., 2005) and the presence of persistent high winds particularly in regions north of the sub-Antarctic front (Jarníková and Tortell, 2016). Around 3.4 Tg of sulfur is released to the atmosphere between December and February, a flux that represents ~15 % of global annual emissions of DMS (Jarníková and Tortell, 2016). Elevated CCN numbers are seen in the most biologically active regions of the Southern Ocean, with a significant contribution from DMS-driven secondary aerosol formation processes (McCoy et al., 2015; Korhonen et al., 2008a). DMS-derived aerosols from this region are estimated to contribute 6 to 10 W m^{-2} to reflected short wavelength radiation, similar to the influence of anthropogenic aerosols in the polluted Northern Hemisphere (McCoy et al., 2015). Given this important influence of polar DMS emissions on atmospheric processes and climate, it is vital we increase our understanding of the influence of future ocean acidification on DMS production.

The polar oceans are characterised by high dissolved inorganic carbon (C_T) concentrations and a low carbonate system buffering capacity, mainly due to the increased solubility of CO_2 in cold waters (Sabine et al., 2004; Orr et al., 2005). This makes these regions particularly susceptible to the impacts of ocean acidification (OA). For example, extensive carbonate mineral undersaturation is expected to occur in Arctic waters within the next 20 – 80 years (McNeil and Matear, 2008; Steinacher et al., 2009). OA has already led to a 0.1 unit decrease in global surface ocean pH, with a further fall of ~0.4 units expected by the end of the century (Orr et al., 2005). The greatest declines in pH are likely in the Arctic Ocean with a predicted fall of 0.45 units by 2100 (Steinacher et al., 2009). OA is occurring at a rate not seen on Earth for 300 Ma, and so the potential effects on marine organisms, communities and ecosystems could be wide-ranging and severe (Raven et al., 2005; Hönisch et al., 2012). Despite the imminent threat to polar ecosystems and the importance of DMS emissions to atmospheric processes, our knowledge of the response of polar DMS production to OA is limited to a single mesocosm experiment performed in a coastal fjord in Svalbard (Riebesell et al., 2013; Archer et al., 2013) and one shipboard microcosm experiment with seawater collected from

Baffin Bay (Hussherr et al., 2017). Both studies reported significant reductions in DMS concentrations with increasing levels of pCO_2 during seasonal phytoplankton blooms. However, these two single studies provide limited information on the wider response of the open Arctic or Southern Oceans.

Mesocosm experiments are a critical tool for assessing OA effects on surface ocean communities. Initial studies focused on the growth and decline of blooms with (Engel et al., 2005; Engel et al., 2008; Schulz et al., 2008; Hopkins et al., 2010; Schulz et al., 2013; Webb et al., 2015; Kim et al., 2006; Kim et al., 2010), or without (Webb et al., 2016; Crawfurd et al., 2016) the addition of inorganic nutrients. The response of DMS to OA has been examined several times, predominantly at the same site in Norwegian coastal waters (Vogt et al., 2008; Hopkins et al., 2010; Webb et al., 2015; Avgoustidi et al., 2012). There have also been two studies in Korean coastal waters (Kim et al., 2010; Park et al., 2014), as well as the single mesocosm study in the coastal (sub) Arctic waters of Svalbard (Archer et al., 2013). Mesocosm enclosures, ranging in volume from ~11,000 – 50,000 L, allow the response of surface ocean communities to a range of CO_2 treatments to be monitored under near-natural light and temperature conditions over time scales (weeks - months) that allow a 'winners vs loser' dynamic to develop. The response of DMS cycling to elevated CO_2 is generally driven by changes to the microbial community structure (Brussaard et al., 2013; Archer et al., 2013; Hopkins et al., 2010; Engel et al., 2008). The size and construction of the mesocosms has limited their deployment to coastal/sheltered waters, resulting in minimal geographical coverage, and leaving large gaps in our understanding of the response of open ocean phytoplankton communities to OA.

Here, we adopt an alternative but complementary approach to explore the effects of OA on the cycling of DMS with the use of short-term shipboard microcosm experiments. We build on the previous temperate NW European shelf studies of Hopkins & Archer (2014) by extending our experimental approach to the Arctic and Southern Oceans. Vessel-based research enables multiple short term (days) near-identical incubations to be performed over extensive spatial scales, that encompass natural gradients in carbonate chemistry, temperature and nutrients (Richier et al., 2014; Richier et al., 2018). This allows an assessment to be made of how a range of surface ocean communities, adapted to a variety of environmental conditions, respond to the same driver. The focus is then on the effect of short-term CO_2 exposure on physiological processes, as well as the extent of the variability in acclimation between communities. The capacity of organisms to acclimate to changing environmental

conditions contributes to the resilience of key ecosystem functions, such as DMS production. Therefore, do spatially-diverse communities respond differently to short term OA, and can this be explained by the range of environmental conditions to which each is presumably already adapted? The rapid CO_2 changes implemented in this study, and during mesocosm studies, are far from representative of the predicted rate of change to seawater chemistry over the coming decades. Nevertheless, our approach can provide insight into the physiological response and level of sensitivity to future OA of a variety of polar surface ocean communities adapted to different in situ carbonate chemistry environments, (Stillman and Paganini, 2015), alongside the implications this may have for DMS production.

Communities of the NW European shelf consistently responded to acute OA with significant increases in net DMS production, likely a result of an increase in stress-induced algal processes (Hopkins and Archer, 2014). Do polar phytoplankton communities, which are potentially adapted to contrasting biogeochemical environments, respond in the same way? By expanding our approach to encompass both polar oceans, we can assess regional contrasts in response. To this end, we combine our findings for temperate waters with those for the polar oceans into a meta-analysis to advance our understanding of the regional variability and drivers in the DMS response to OA.

2 Material and Methods

2.1 Sampling stations

This study presents new data from two sets of field experiments carried out as a part of the UK Ocean Acidification Research Programme (UKOA) aboard the RRS James Clark Ross in the sub-Arctic and Arctic in June-July 2012 (JR271) and in the Southern Ocean in January-February 2013 (JR274). Data are combined with the results from an earlier study on board the RRS Discovery (D366) described in Hopkins & Archer (2014) performed in the temperate waters of the NW European shelf. Additionally, four previously unpublished experiments from D366 are also included (E02b, E04b, E05b, E06) as well as two temperate experiments from JR271 (NS and IB) (see Table 1). In total, 18 incubations were performed; 11 in temperate and sub-Arctic waters of the NW European shelf and North Atlantic, 3 in Arctic waters and 4 in the Southern Ocean. Figure 1 shows the cruise tracks, surface concentrations of DMS and total DMSP (DMSPt) at CTD sampling stations as well as the locations of sampling for shipboard microcosms (See Table 1 for further details).

2.2 Shipboard microcosm experiments

The general design and implementation of the experimental microcosms for JR271 and JR274 was essentially the same as for D366 and described in Richier et al. (2014), (2018) and Hopkins & Archer (2014), but with the additional adoption of trace metal clean sampling and incubation techniques in the low trace metal open ocean waters (see Richier et al. (2018)). At each station, pre-dawn vertical profiles of temperature, salinity, oxygen, fluorescence, turbidity and irradiance were used to choose and characterise the depth of experimental water collection. Subsequently, water was collected within the mixed layer from three successive separate casts of a trace-metal clean titanium CTD rosette comprising twenty-four 10 L Niskin bottles. Each cast was used to fill one of a triplicated set of experimental bottles (locations and sample depths, Table 1). Bottles were sampled within a class-100 filtered air environment within a trace metal clean container to avoid contamination during the set up. The water was directly transferred into acid-cleaned 4.5 L polycarbonate bottles using acid-cleaned silicon tubing, with no screening or filtration.

The carbonate chemistry within the experimental bottles was manipulated by addition of equimolar HCl and $NaHCO_3^-$ (1 mol L^{-1}) to achieve a range of target CO_2 values (550, 750, 1000, 2000 µatm) (Gattuso et al., 2010). For the sub-Arctic/Arctic microcosms, additions were used to attain three target CO_2 levels (550 µatm, 750 µatm and 1000 µatm). For Southern Ocean experiments, two experiments (*Drake Passage* and *Weddell Sea*) underwent combined CO_2 and Fe additions (ambient, Fe (2 nM), high CO_2 (750 µatm), Fe (2 nM) + high CO_2 (750µatm) (only high CO_2 treatments will be examined here; no response to Fe was detected in DMS or DMSP concentrations). Three CO_2 treatments (750 µatm, 1000 µatm, 2000 µatm) were tested in the last two experiments (*South Georgia* and *South Sandwich*). Full details of the carbonate chemistry manipulations can be found in Richier et al. (2014) and Richier et al. (2018). Broadly, achieved pCO_2 levels were well-matched to target values at T_0, although differences in pCO_2 between target and initial values were greater in the higher pCO_2 treatments, due to lowered carbonate system buffer capacity at higher pCO_2. For all 18 experiments, actual attained pCO_2 values were on average around 89% ± 12% (± 1 SD) of target values. The attained pCO_2 values are presented in Table S1 on the Supplementary Information. For simplicity, experimental data is presented against its target ('nominal') pCO_2 treatment throughout the paper. After first ensuring the absence of bubbles or headspace, the bottles were sealed with high density polyethylene (HDPE) lids with silicone/ polytetrafluoroethylene (PTFE) septa and placed in the incubation container. Bottles were

incubated inside a custom-designed temperature- and light-controlled shipping container, set to match (±<1°C) the *in situ* water temperature at the time of water collection (shown in Table 1) (see Richier et al. 2018). A constant light level (100 µE m^{-2} s^{-1}) was provided by daylight simulating LED panels (Powerpax, UK). The light period within the microcosms was representative of *in situ* conditions. For the sub-Arctic/Arctic Ocean stations, experimental bottles were subjected to continuous light representative of the 24 h daylight of the Arctic summer. For Southern Ocean and all temperate water stations, an 18:6 light: dark cycle was used. Each bottle belonged to a set of triplicates, and sacrificial sampling of bottles was performed (see Table 1 for chosen time points). Use of three sets of triplicates for each time point allowed for the sample requirements of the entire scientific party (3 x 3 bottles, x 2 time points (T_1, T_2, see Table 1 for specific times for each experiment), x 4 CO_2 treatments = 72 bottles in total). Experiments were generally run for ≥4 days (15 out of 18 experiments), with initial sampling proceeded by two further time points. For three temperate experiments (E02b, E04b, E05b, see Table 1) a shorter 2 day incubation was performed, with a single sampling point at the end. For E06 (see Table 1) high time frequency sampling was performed (0, 1, 4, 14, 24, 48, 72, 96 h) although only the data at 48 h and 96 h is considered in this analysis. Incubation times were extended for Southern Ocean stations *Weddell Sea*, *South Georgia* and *South Sandwich* (see Table 1) as minimal CO_2 response, attributed to slower microbial metabolism at low water temperatures, was observed for Arctic stations and the first Southern Ocean station *Drake Passage*. The magnitude of response was not related to incubation times, and expected differences in net growth rates (2- to 3-fold higher in temperate compared to polar waters (Eppley, 1972)) did not account for the differences in response magnitude despite the increased incubation time in polar waters (see Richier et al. (2018) for detailed discussion). Samples for carbonate chemistry measurements were taken first, followed by sampling for DMS, DMSP and related parameters.

2.3 Standing stocks of DMS and DMSP

Methods for the determination of seawater concentrations of DMS and DMSP are identical to those described in Hopkins & Archer (2014) and will therefore be described in brief here. Seawater DMS concentrations were determined by cryogenic purge and trap, with gas chromatography and pulsed flame photometric detection (Archer et al., 2013). Samples for total DMSP concentrations were fixed by addition of 35 µl of 50 % H_2SO_4 to 7 mL of seawater (Kiene and Slezak, 2006), and analysed within 2 months of collection (Archer et al.,

2013). Concentrations of DMSPp were determined at each time point by gravity filtering 7 ml of sample onto a 25 mm GF/F filter and preserving the filter in 7 ml of 35 mM H_2SO_4 in MQ-water. DMSP concentrations were subsequently measured as DMS following alkaline hydrolysis. DMS calibrations were performed using alkaline cold-hydrolysis (1 M NaOH) of DMSP sequentially diluted three times in MilliQ water to give working standards in the range 0.03 – 3.3 ng S mL^{-1}. Five point calibrations were performed every 2 – 4 days throughout the cruise.

2.4 *De novo* DMSP synthesis

De novo DMSP synthesis and gross production rates were determined for all microcosm experiments, except *Barents Sea* and *South Sandwich*, at each experimental time point, using methods based on the approach of Stefels et al. (2009) and described in detail in Archer et al. (2013) and Hopkins and Archer (2014). Triplicate rate measurements were determined for each CO_2 level. For each rate measurement three x 500 mL polycarbonate bottles were filled by gently siphoning water from each replicate microcosm bottle. Trace amounts of $NaH^{13}CO_3$, equivalent to ~6 % of *in situ* dissolved inorganic carbon (C_T), were added to each 500 mL bottle. The bottles were incubated in the microcosm incubation container with temperature and light levels as described earlier. Samples were taken at 0 h, then at two further time points over a 6 - 9 h period. At each time point, 250 mL was gravity filtered in the dark through a 47 mm GF/F filter, the filter gently folded and placed in a 20 mL serum vial with 10 mL of Milli-Q and one NaOH pellet, and the vial was crimp-sealed. Samples were stored at -20°C until analysis by proton transfer reaction-mass spectrometer (PTR-MS) (Stefels et al. 2009).

The specific growth rate of DMSP (μDMSP) was calculated assuming exponential growth from:

$$\mu_t(\Delta t^{-1}) = \alpha_k \text{ x AVG}\left[\ln\left(\frac{^{64}MP_{eq} - {}^{64}MP_{t-1}}{^{64}MP_{eq} - {}^{64}MP_{t}}\right), \ln\left(\frac{^{64}MP_{eq} - {}^{64}MP_{t}}{^{64}MP_{eq} - {}^{64}MP_{t+1}}\right)\right] \quad (1)$$

(Stefels et al. 2009) where $^{64}MP_t$, $^{64}MP_{t-1}$, $^{64}MP_{t+1}$ are the proportion of 1 x ^{13}C labelled DMSP relative to total DMSP at time t, at the preceding time point (t-1) and at the subsequent time point (t+1), respectively. Values of ^{64}MP were calculated from the protonated masses of DMS as: mass 64/(mass63+mass64+mass65), determined by PTR-MS. $^{64}MP_{eq}$ is the

theoretical equilibrium proportion of 1 x ^{13}C based on a binomial distribution and the proportion of tracer addition. An isotope fractionation factor α_k of 1.06 is included, based on laboratory culture experiments using *Emiliania huxleyi* (Stefels et al. 2009). Gross DMSP production rates during the incubations (nmol L^{-1} h^{-1}) were calculated from μDMSP and the initial particulate DMSP (DMSPp) concentration of the incubations (shown in Figure 4).

2.5 Seawater carbonate chemistry analysis

The techniques and methods used to determine both the *in situ* and experimental carbonate chemistry parameters, and to manipulate seawater carbonate chemistry within the microcosms, are described in Richier et al. (2014) and will be only given in brief here. Experimental T_0 measurements were taken directly from CTD bottles, and immediately measured for total alkalinity (A_T) (Apollo SciTech AS-Alk2 Alkalinity Titrator) and dissolved inorganic carbon (C_T) (Apollo SciTech C_T analyser (AS-C3) with LICOR 7000). The CO2SYS programme (version 1.05) (Lewis and Wallace, 1998) was used to calculate the remaining carbonate chemistry parameters including pCO_2.

Measurements of T_A and C_T were made from each bottle at each experimental time point and again used to calculate the corresponding values for pCO_2 and pH_T. The carbonate chemistry data for each sampling time point for each experiment are summarised in Supplementary Table S1, S2 and S3 (Experimental starting conditions are given in Table 1).

2.6 Chlorophyll a (Chl *a*) determinations

Concentrations of Chl *a* were determined as described in Richier et al. (2014). Briefly, 100 mL aliquots of seawater from the incubation bottles were filtered through either 25 mm GF/F (Whatman, 0.7 μm pore size) or polycarbonate filters (Whatman, 10 μm pore size) to yield total and >10 μm size fractions, with the <10 μm fraction calculated by difference. Filters were extracted in 6 mL HPLC-grade acetone (90%) overnight in a dark refrigerator. Fluorescence was measured using a Turner Designs Trilogy fluorometer, which was regularly calibrated with dilutions of pure Chl *a* (Sigma, UK) in acetone (90%).

2.8 Community composition

Composition of small phytoplankton community compostion was assessed by flow cytometry. For details of methodology, see Richier et al. (2014).

2.9 Data handling and statistical analyses

Permutational analysis of variance (PERMANOVA) was used to analyse the difference in response of DMS and DMSP concentrations to OA, both between and within the two polar cruises in this study. Both dependant variables were analysed separately using a nested factorial design with three factors; (i) Cruise Location: Arctic and Southern Ocean, (ii) Experiment location nested within Cruise location (see Table 1 for station IDs) and (iii) CO_2 level: 385, 550, 750, 1000 and 2000 µatm. Main effects and pairwise comparisons of the different factors were analysed through unrestricted permutations of raw data. If a low number of permutations were generated then the *p*-value was obtained through random sampling of the asymptotic permutation distribution, using Monte Carlo tests.

One-way analysis of variance was used to identify differences in ratio of >10 µm Chl *a* to total Chl *a* ($chl_{>10um}$: chl_{tot} , see Discussion). Initially, tests of normality were applied ($p<0.05$ = not normal), and if data failed to fit the assumptions of the test, linearity transformations of the data were performed (logarithmic or square root), and the ANOVA proceeded from this point. The results of ANOVA are given as follows: *F* = ratio of mean squares, *df* = degrees of freedom, *p* = level of confidence. For those data still failing to display normality following transformation, a rank-based Kruskal-Wallis test was applied (*H* = test statistic, *df* = degrees of freedom, *p* = level of confidence).

3 Results

3.1 Sampling stations

At temperate sampling stations, sea surface temperatures ranged from 10.7°C for *Iceland Basin*, to 15.3°C for *Bay of Biscay*, with surface salinity in the range 34.1 – 35.2, with the exception of station E05b which had a relatively low salinity of 30.5 (Figure 2 and Table 1). Seawater temperatures at the polar microcosm sampling stations ranged from -1.5°C at sea-ice influenced stations (*Greenland Ice-edge* and *Weddell Sea*) up to 6.5°C for *Barents Sea* (Fig. 2 A). Salinity values at all the Southern Ocean stations were <34, whilst they were ~35 at all the Arctic stations with the exception of *Greenland Ice-edge* which had the lowest salinity of 32.5 (Fig. 2 B). Phototrophic nanoflagellate abundances were variable, with >3 x 10^4 cells mL^{-1} at *Greenland Gyre*, 1.5 x 10^4 cells mL^{-1} at *Barents Sea* and <3 x 10^3 cells mL^{-1} for all other stations (Fig. 2 D). Total bacterial abundances ranged from 3 x 10^5 cells mL^{-1} at *Greenland Ice-edge* up to 3 x 10^6 cells mL^{-1} at *Barents Sea* (Fig. 2 E).

Chl *a* concentrations in temperate waters ranged from 0.3 µg L^{-1} for two North Sea stations (*E05* and *North Sea*) up to 3.5 µg L^{-1} for *Irish Sea* (Figure 2 and Table 1). Chl a was also variable in polar waters, exceeding 4 µg L^{-1} at *South Sandwich* and 2 µg L^{-1} at *Greenland Ice-edge*, whilst the remaining stations ranged from 0.2 µg L^{-1} (*Weddell Sea*) to 1.5 µg L^{-1} (Figure 2). The high Chl *a* concentrations at *South Sandwich* are reflected in low in-water irradiance levels at this station (Fig. 2 C).

In temperate waters, maximum DMS concentrations were generally seen in near surface measurements, ranging from 1.0 nM for *E04* to 21.1 nM for *E06*, with rapidly decreasing concentrations with depth (Figure 2 G). DMSP also generally peaked in the near surface waters, ranging from 12.0 nM for E04 to 72.5 nM for *E06*, but the maximum overall DMSP concentration of 89.8 nM was observed at ~20 m for *E05b* (Figure 2 H). Surface DMS concentrations in polar waters were generally lower than temperate waters, ranging from 1 – 3 nM, with the exception of *South Sandwich* where concentrations of ~12 nM were observed (Figure 2 G). DMSP generally ranged from 12 – 20 nM[1], except *Barents Sea* where surface concentrations exceeded 60 nM (Figure 2 H).

3.2 Response of DMS and DMSP to OA

The temporal trend in DMS concentrations showed a similar pattern for the three Arctic Ocean experiments. Initial concentrations of 1 – 2 nmol L^{-1} remained relatively constant over the first 48 h and then showed small increases of 1 - 4 nmol L^{-1} over the incubation period (Figure 3 A – C). Increased variability between triplicate incubations became apparent in all three Arctic experiments by 96 h, but no significant effects of elevated CO_2 on DMS concentrations were observed. Initial DMSP concentrations were more variable, from 6 nmol L^{-1} at *Greenland Ice-edge* to 12 nmol L^{-1} at *Barents Sea*, and either decreased slightly (net loss 1 – 2 nmol L^{-1} GG), or increased slightly (net increase ~4 nmol L^{-1} *Greenland Ice-edge*, ~3 nmol L^{-1} *Barents Sea*) (Figure 4 A – C). DMSP concentrations were found to decrease significantly in response to elevated CO_2 after 48 h for *Barents Sea* (Fig. 4 C, $t = 2.05$, $p = 0.025$), whist no significant differences were seen after 96 h. No other significant responses in DMSP were identified.

The range of initial DMS concentrations was greater at Southern Ocean sampling stations compared to the Arctic, from 1 nmol L^{-1} at *Drake Passage* up to 13 nmol L^{-1} at *South Sandwich* (Figure 3 D – G). DMS concentrations showed little change over the course of 96 – 168 h incubations and no effect of elevated CO_2, with the exception of *South Sandwich* (Fig.

3 G). Here, concentrations decreased sharply after 96 h by between 3 and 11 nmol L^{-1}. Concentrations at 96 h were CO_2-treatment dependent, with significant decreases in DMS concentration occurring with increasing levels of CO_2 (PERMANOVA, $t = 2.61$, $p = 0.028$). Significant differences ceased to be detectable by the end of the incubations (168 h). Initial DMSP concentrations were higher at the Southern Ocean stations than for Arctic stations, ranging from 13 nmol L^{-1} for *Weddell Sea* to 40 nmol L^{-1} for *South Sandwich* (Figure 4 D – G). Net increases in DMSP occurred throughout, except at South Georgia, and were on the order of between <10 nmol L^{-1} - >30 nmol L^{-1} over the course of the incubations. Concentrations were not generally pCO_2-treatment dependent with the exception of the final time point at *South Georgia* (144 h) when a significantly lower DMSP with increasing CO_2 was observed (PERMANOVA, $t = -5.685$, $p<0.001$).

Results from the previously unpublished experiments from temperate waters are in strong agreement with the five experiments presented in Hopkins and Archer (2014), with consistently decreased DMS concentrations and enhanced DMSP under elevated CO_2. The data is presented in the Supplementary Information, Table S4 and Figure S2, and included in the meta-analysis in section 4.1 of this paper.

3.3 Response of de novo DMSP synthesis and production to OA

Rates of *de novo* DMSP synthesis (μDMSP) at initial time points (T_0) ranged from 0.13 d^{-1} (*Weddell Sea*, Fig. 5 G) to 0.23 d^{-1} (*Greenland Ice-edge*, Fig. 5 C), whilst DMSP production ranged from 0.4 nmol L^{-1} d^{-1} (*Greenland Gyre*, Fig. 5 B) to 2.27 nmol L^{-1} d^{-1} (*Drake Passage*, Fig. 5 F). Maximum rates of μDMSP of 0.37 -0.38 d^{-1} were observed at *Greenland Ice-edge* after 48 h of incubation in all CO_2 treatments (Fig. 5 C). The highest rates of DMSP production were observed at *South Georgia* after 96 h of incubation, and ranged from 4.1 – 6.9 nmol L^{-1} d^{-1} across CO_2 treatments (Fig. 5 J). Rates of DMSP synthesis and production were generally lower than those measured in temperate waters (Hopkins and Archer, 2014) (Initial rates: μDMSP 0.33 – 0.96 d^{-1}, 7.1 – 37.3 nmol L^{-1} d^{-1}), but were comparable to measurements made during an Arctic mesocosm experiment (Archer et al., 2013) (0.1 – 0.25 d^{-1}, 3 – 5 nmol L^{-1} d^{-1} in non-bloom conditions). The lower rates in cold polar waters likely reflect slower metabolic processes and are reflected by standing stock DMSP concentrations which were also lower than in temperate waters (5 – 40 nmol L^{-1} polar, 8 – 60 nmol L^{-1} temperate (Hopkins and Archer, 2014)). No consistent evidence of CO_2 sensitivity was seen in either DMSP synthesis or production, similar to findings for DMSP standing stocks. Some

notable but conflicting differences between CO_2 treatments were observed. There was a 36% and 37% increase in µDMSP and DMSP production respectively at 750 µatm for the *Drake Passage* after 96 h (Figure 5 E, F), and a 38% and 44% decrease in both at 750 µatm after 144 h for *Weddell Sea* (Figure 5 G, H). Nevertheless, no consistent and significant effects of high CO_2 were observed for rates of *de novo* DMSP synthesis or DMSP production in polar waters.

4 Discussion

4.1 Regional differences in the response of DMS(P) to OA

We combine our findings from the polar oceans with those from temperate waters into a meta-analysis in order to assess the regional variability and drivers in the DMS(P) response to OA. Figures 6 and 7 provide an overview of the results discussed so far in this current study, together with the results from Hopkins & Archer (2014) as well as the results from 4 previously unpublished microcosm experiments from the NW European shelf cruise and a further 2 temperate water microcosm experiments from the Arctic cruise (*North Sea* and *Iceland Basin*, Table 1). This gives a total of 18 microcosm experiments, each with between 1 and 3 high CO_2 treatments.

Hopkins & Archer (2014) reported consistent and significant increases in DMS concentration in response to elevated CO_2 that were accompanied by significant decreases in DMSPt concentrations. Bacterially-mediated DMS processes appeared to be insensitive to OA, with no detectable effects on dark rates of DMS consumption and gross production, and no consistent response seen in bacterial abundance (Hopkins and Archer, 2014). In general, there were large short-term decreases in Chl *a* concentrations and phototrophic nanoflagellate abundance in response to elevated CO_2 in these experiments (Richier et al., 2014).

The relative treatment effects ($[x]_{highCO2}/[x]_{ambientCO2}$) for DMS and DMSP (Figure 6), Chl *a* and phototrophic nanoflagellate abundance (Figure 8) are plotted against the ratio of C_T to A_T (C_T/A_T) of the sampled waters, in order to place our findings in context of the total experimental data set. The value of C_T/A_T ranges from 0.84 – 0.95 within the mixed layer, and increases towards high latitude waters (Egleston et al., 2010). Thus, stations with C_T/A_T above ~0.91 represent the seven polar stations (right of red dashed line Fig. 6 and 7). The surface waters of the polar oceans have a reduced buffering capacity due to higher CO_2 solubility in colder waters, and so are less resistant to local variations in C_T and A_T (Sabine et

al., 2004). Thus, the relationship between experimental response and C_T/A_T is a simple way of demonstrating how the CO_2 sensitivity of different surface ocean communities relates to the *in situ* carbonate chemistry. The effect of elevated CO_2 on DMS concentrations at polar stations, relative to ambient controls, was minimal at all sampling points, and is in strong contrast to the results from experiments performed on the NW European shelf. At temperate stations, DMSP displayed a clear negative treatment effect, whilst at polar stations a positive effect was evident under high CO_2, and particularly at T_1 (48 – 96 h) (Fig. 6 C and D). *De novo* DMSP synthesis and DMSP production rates show a similar relationship with C_T/A_T (Fig. 7 A and B), with a significant suppression of DMSP production rates in temperate waters compared to polar waters (Fig. 7B, Kruskal-Wallis One Way ANOVA $H = 8.711$, $df = 1$, $p = 0.003$). Although a similar trend was seen for *de novo* DMSP synthesis, the difference between temperate and polar waters was not statistically significant (Fig. 7A). At T_1 (48 – 96 h, see Table 1), a statistically significant difference in response was seen between temperate and polar waters for Chl *a* (Kruskal-Wallis One Way ANOVA $H = 20.577$, $df = 1$, $p<0.001$), with minimal response to elevated CO_2 at polar stations, and in general a strong negative response was seen in temperate waters (Fig. 8A). By T_2 (96 – 144 h, see Table 1), no significant difference in response of Chl *a* between temperate and polar waters was detectable (Fig. 8B), although a slight positive response in Chl *a* was seen at some temperate stations, and polar stations showed a minimal response, with the exception of *Barents Sea* which saw strongly enhanced Chl *a* at T_2 (96 h) (Fig. 8 B).

In general, phototrophic nanoflagellates responded to high CO_2 with large decreases in abundance in temperate waters (Richier et al. 2014), and increases in abundance in polar waters (Fig. 8 C and D), with some exceptions: *North Sea* and *South Sandwich* gave the opposite response. The impacts had lessened by T_2 (96 – 168 h, see Table 1). In contrast, bacterial abundance did not show the same regional differences in response to high CO_2 (see Hopkins and Archer (2014) for temperate waters, and Figure S1, supplementary information, for polar waters). Bacterial abundance in temperate waters gave variable and inconsistent responses to high CO_2. For all Arctic stations, *Drake Passage* and *Weddell Sea*, no response to high CO_2 was observed. For *South Georgia* and *South Sandwich*, bacterial abundance increased at 1000 and 2000 µatm, with significant increases for *South Georgia* after 144 h of incubation (ANOVA $F = 137.936$, $p<0.001$). Additionally, at Arctic stations *Greenland Gyre* and *Greenland Ice-edge*, no overall effect of increased CO_2 on rates of DOC release, total carbon fixation or POC : DOC was observed (Poulton et al., 2016).

Across all experiments, the response of net total community Chl *a* and net growth rates of small phytoplankton (<10 μm) scaled with pCO_2 treatment, and strongly correlated with in situ carbonate chemistry, whilst no relationships were found with any of the other wide range of initial physical, chemical or biological variables (Richier et al. 2018). Overall, the observed differences in regional response to carbonate chemistry manipulation could not be attributed to any other measured factor that varied systematically between temperate and polar waters. These include ambient nutrient concentrations, which varied considerably but where direct manipulation had no influence on the response, and initial community structure, which was not a significant predictor of the response (Richier et al. 2018).

In summary, the relative response in both DMS(P) and a range of biological parameters (Richier et al. 2018) to CO_2 treatment in polar waters follows a distinctly different pattern to experiments performed in temperate waters. In the following sections we explore the possible drivers of the regional variability in response to OA.

4.2 Influence of community cell-size composition on DMS response

It has been proposed that variability in the concentrations of carbonate species (e.g. pCO_2, HCO_3^-, CO_3^{2-}) experienced by phytoplankton is related to cell size, such that smaller-celled taxa (<10 μm) with a reduced diffusive boundary layer are naturally exposed to relatively less variability compared to larger cells (Flynn et al., 2012). Thus, short-term and rapid changes in carbonate chemistry, such as the kind imposed during our microcosm experiments, may have a disproportionate effect on the physiology and growth of smaller celled species. Larger cells may be better able to cope with variability as normal cellular metabolism results in significant cell surface changes in carbonate chemistry parameters (Richier et al., 2014). Indeed, the marked response in DMS concentrations to short term OA in temperate waters has been attributed to this enhanced sensitivity of small phytoplankton (Hopkins and Archer, 2014). Was the lack of DMS response to OA in polar waters therefore a result of the target communities being dominated by larger-celled, less carbonate-sensitive species?

Size-fractionated Chl *a* measurements give an indication of the relative contribution of large and small phytoplankton cells to the community. For experiments in temperate waters, the mean ratio of >10 μm Chl *a* to total Chl *a* (hereafter *>10 μm : total*) of 0.32 ± 0.08 was lower than the ratio for polar stations of 0.54 ± 0.13 (Table 2). Although the difference was not statistically significant, this might imply a tendency towards communities dominated by

larger cells in the polar oceans, which may partially explain the apparent lack of DMS response to elevated CO_2. However, this is not a consistent explanation for the observed responses. For example, the Arctic *Barents Sea* station had the lowest observed *>10 μm : total* of 0.04 ± 0.01, suggesting a community comprised almost entirely of <10 μm cells; yet the response to short term OA differed to the response seen in temperate waters. No significant CO_2 effects on DMS or DMSP concentrations or production rates were observed at this station, whilst total Chl *a* significantly increased under the highest CO_2 treatments after 96 h (PERMANOVA $F = 33.239$, $P<0.001$). Thus, our cell size theory does not hold for all polar waters, suggesting that regardless of the dominant cell size, polar communities are more resilient to OA. In the following section, we explore the causes of this apparent insensitivity to OA in terms of the environmental conditions to which the communities have presumably adapted.

4.3 Adaptation to a variable carbonate chemistry environment

The variation in *in situ* surface ocean carbonate chemistry parameters for all three cruises (see Tynan et al. 2016 for details), is summarised in Figure 9. These data demonstrate both the latitudinal differences in surface ocean carbonate chemistry between temperate and polar waters, as well as the within-region variability which is controlled by the respective buffer capacities. Thus, a narrow range of values for all carbonate parameters was observed in the NW European shelf waters relative to the less well-buffered Arctic and Southern Ocean waters. The polar waters sampled during our study were characterised by pronounced gradients in carbonate chemistry over small spatial scales, such that surface ocean communities are more likely to have experienced fluctuations between high $pH/\Omega_{aragonite}$ and low $pH/\Omega_{aragonite}$ over short time scales (Tynan et al., 2016). For example, pH_T varied by only 0.15 units (8.20 - 8.05) in NW European shelf waters, compared to 0.35 units (8.05 - 7.7) in the Arctic, and 0.40 units (8.25 - 7.85) in the Southern Ocean. Although it might be expected that carbonate system variability on the level 'experienced' by the cells, i.e. ~daily cellular level variability, might be the most important factor driving sensitivity (Flynn et al. 2012; Richier et al. 2018), our data represent only a snapshot (4 – 6 weeks) of a year, and thus do not contain information on the range in variability over seasonal cycles. For comparison with Arctic stations, Hagens and Middelburg (2016) report a seasonal pH variability of up to 0.25 units from a single site in the open ocean surface waters in the Iceland Sea, whilst Kapsenberg et al. (2015) report an annual variability of 0.3 – 0.4 units in the McMurdo

505 Sound, Antarctica. This implies that both polar open ocean and coastal/sea ice locations
506 experience equally large variations in carbonate chemistry over seasonal cycles. In open
507 ocean waters this is driven by enhanced drawdown of C_T and CO_2 during the productive
508 spring and summer months, countered by lower productivity and strong mixing in the winter
509 (Hagens and Middelburg, 2016). In coastal and sea-ice affected regions, seasonal pH
510 variability may be enhanced further by tidal exchanges, and by dilution of C_T/A_T caused by
511 sea-ice melt (Kapsenberg et al., 2015). Adaptation to such natural variability may induce the
512 ability to resist abrupt changes within the polar biological community (Kapsenberg et al.,
513 2015). This is manifested here as negligible impacts on rates of *de novo* DMSP synthesis and
514 net DMS production. A number of previous studies in polar waters have reported similar
515 findings. Phytoplankton communities were able to tolerate a pCO_2 range of 84 – 643 µatm in
516 ~12 d minicosm experiments (650 L) in Antarctic coastal waters, with no effects on
517 nanophytoplankton abundance, and enhanced abundance of picophytoplankton and
518 prokaryotes (Davidson et al., 2016;Thomson et al., 2016). In experiments under the Arctic
519 ice, microbial communities demonstrated the capacity to respond either by selection or
520 physiological plasticity to elevated CO_2 during short term experiments (Monier et al., 2014).
521 Subarctic phytoplankton populations demonstrated a high level of resilience to OA in short
522 term experiments, suggesting a high level of physiological plasticity that was attributed to the
523 prevailing strong gradients in pCO_2 levels experienced in the sample region (Hoppe et al.,
524 2017). Furthermore, a more recent study describing ten CO_2 manipulation experiments in
525 Arctic waters found that primary production was largely insensitive to OA over a large range
526 of light and temperature levels (Hoppe et al., 2018). This supports our hypothesis that,
527 relative to temperate communities, polar microbial communities may have a high capacity to
528 compensate for environmental variability (Hoppe et al., 2018), and are thus already adapted
529 to, and are able to tolerate, large variations in carbonate chemistry. Thus by performing
530 multiple, replicated experiments over a broad geographic range, the findings of this study
531 imply that the DMS response may be both a reflection of: (i) the level of sensitivity of the
532 community to changes in the mean state of carbonate chemistry, and (ii) the levels of regional
533 variability in carbonate chemistry experienced by different communities. This highlights the
534 limitations associated with simple extrapolation of results from a small number of
535 geographically-limited experiments e.g. Six et al. (2013). Such an approach lacks a
536 mechanistic understanding that would allow a model to capture the regional variability in
537 response that is apparent from the microcosms experiments presented here.

4.4 Comparison to an Arctic mesocosm experiment

Experimental data clearly provide useful information on the potential future DMS response to OA, but these data become most powerful when incorporated in Earth System Models (ESM) to facilitate predictions of future climate. To date, two modelling studies have used ESM to assess the potential climate feedback resulting from the DMS sensitivity to OA (Six et al., 2013;Schwinger et al., 2017), and both have used results from mesocosm experiments. However, the DMS responses to OA within our short term microcosm experiments contrast with the results of most previous mesocosm experiments, and of particular relevance to this study, an earlier Arctic mesocosm experiment (Archer et al., 2013). Whilst no response in DMS concentrations to OA was generally seen in the microcosm experiments discussed here, a significant decrease in DMS with increasing levels of CO_2 in the earlier mesocosm study was seen. Therefore, it is useful to consider how the differences in experimental design between microcosms and mesocosms may result in contrasting DMS responses to OA.

The short duration of the microcosm experiments (4 – 7 d) allows the physiological (phenotypic) capacity of the community to changes in carbonate chemistry to be assessed. In other words, how well is the community adapted to variable carbonate chemistry and how does this influence its ability to acclimate to change? Although the mesocosm experiment considered a longer time period (4 weeks), the first few days can be compared to the microcosms. No differences in DMS or DMSP concentrations were detected for the first week of the mesocosm experiment, implying a certain level of insensitivity of DMS production to the rapid changes in carbonate chemistry. In fact, when taking all previous mesocosm experiments into consideration, differences in DMS concentrations have consistently been undetectable during the first 5 – 10 days, implying there is a limited short-term physiological response by the in situ communities (Hopkins et al., 2010b;Avgoustidi et al., 2012;Vogt et al., 2008;Kim et al., 2010;Park et al., 2014). This is in contrast to the strong response in the temperate microcosms from the NW European shelf (Hopkins and Archer, 2014). However, all earlier mesocosm experiments have been performed in coastal waters, which like polar waters, can experience a large natural range in carbonate chemistry. In the case of coastal waters this is driven to a large extent by the influence of riverine discharge and biological activity (Fassbender et al., 2016). Thus coastal communities may also possess a higher level of adaptation to variable carbonate chemistry compared to the open ocean communities of the temperate microcosms (Fassbender et al., 2016).

570 The later stages of mesocosm experiments address a different set of hypotheses, and are less
571 comparable to the microcosms reported here. With time, an increase in number of generations
572 leads to community structure changes and taxonomic shifts, driven by selection on the
573 standing genetic variation in response to the altered conditions. Moreover, the coastal Arctic
574 mesocosms were enriched with nutrients after 10 days, affording relief from nutrient
575 limitation and allowing differences between pCO_2 treatments to be exposed, including a
576 strong DMS(P) response.(Archer et al., 2013;Schulz et al., 2013). During this period of
577 increased growth and productivity, CO_2 increases drove changes which reflected both the
578 physiological and genetic potential within the community, and resulted in taxonomic shifts.
579 The resultant population structure was changed, with an increase in abundance of
580 dinoflagellates, particularly *Heterocapsa rotundata*. Increases in DMSP concentrations and
581 DMSP synthesis rates were attributed to the population shift towards dinoflagellates. The
582 drivers of the reduced DMS concentrations were less clear, but may have been linked to
583 reduced DMSP-lyase capacity within the dominant phytoplankton, a reduction in bacterial
584 DMSP lysis, or an increase in bacterial DMS consumption rates (Archer et al., 2013). Again,
585 this is comparable to all other mesocosm experiments, wherein changes to DMS
586 concentrations can be associated with CO_2-driven shifts in community structure (Hopkins et
587 al., 2010b;Avgoustidi et al., 2012;Vogt et al., 2008;Kim et al., 2010;Park et al., 2014;Webb et
588 al., 2015). However, given the lack of further experiments of a similar location, design and
589 duration to the Arctic mesocosm, it is unclear how representative the mesocosm result is of
590 the general community-driven response to OA in high latitude waters.

591 We did not generally see any broad-scale CO_2-effects on community structure in polar
592 waters. This can be demonstrated by a lack of significant differences in the mean ratio of >10
593 µm Chl *a* to total Chl *a* (*>10 µm : total*) between CO_2 treatments, implying there were no
594 broad changes in community composition (Table 2). *South Sandwich* was an exception to
595 this, where large and significant increases in the mean ratio of *>10 µm : total* were observed
596 at 750 µatm and 2000 µatm CO_2 relative to ambient CO_2 (ANOVA, $F = 207.144$, $p<0.001$, $df = 3$), demonstrated at even the short timescale of the microcosm experiments, it is possible
598 for some changes to community composition to occur. Interestingly, this was also the only
599 polar station that exhibited any significant effects on DMS after 96 h of incubation (Figure
600 3G). However, given the lack of similar response at 1000 µatm, it remains equivocal whether
601 this was driven by a CO_2-effect or some other factor. The results of our microcosm
602 experiments suggest insensitivity of *de novo* DMSP production and net DMS production in

603 the microbial communities of the polar open oceans to short term changes in carbonate
604 chemistry. This may be driven by a high level of adaptation within the targeted
605 phytoplankton communities to naturally varying carbonate chemistry.

606 In contrast to our findings, a recent single 9 day microcosm experiment (Hussherr et al.,
607 2017) performed in Baffin Bay (Canadian Arctic) saw a linear 80% decrease in DMS
608 concentrations during spring bloom-like conditions. It should be noted that this response was
609 seen over a range of pCO_2 from 500 - 3000 µatm, far beyond the levels used in the present
610 study. Nevertheless, this implies that polar DMS production may be sensitive to OA at certain
611 times of the year, such as during the highly productive spring bloom, but less sensitive during
612 periods of low and stable productivity, such as the summer months sampled during this study.
613 Furthermore, a number of other studies from both the Arctic e.g. (Coello-Camba et al.,
614 2014;Holding et al., 2015;Thoisen et al., 2015) and the Southern Ocean e.g. (Trimborn et al.,
615 2017;Tortell et al., 2008;Hoppe et al., 2013) suggest that polar phytoplankton communities
616 can demonstrate sensitivity to OA, in contrast to our findings. This emphasises the need to
617 gain a more detailed understanding of both the spatial and seasonal variability in the polar
618 phytoplankton community and associated DMS response to changing ocean acidity.

619 ## 5 Conclusions

620 We have shown that net DMS production by summertime polar open ocean microbial
621 communities is insensitive to OA during multiple, highly replicated short term microcosm
622 experiments. We provide evidence that, in contrast to temperate communities (Hopkins and
623 Archer, 2014), the polar communities we sampled were relatively insensitive to variations in
624 carbonate chemistry (Richier et al., 2018), manifested here as a minimal effect on net DMS
625 production. Our findings contrast with two previous studies performed in Arctic waters
626 (Archer et al. 2013; Hussherr et al. 2017) which showed significant decreases in DMS in
627 response to OA. These discrepancies may be driven by differences in the sensitivity of
628 microbial communities to changing carbonate chemistry between different areas, or by
629 variability in the response to OA depending on the time of year, nutrient availability, and
630 ambient levels of growth and productivity. This serves to highlight the complex spatial and
631 temporal variability in DMS response to OA which warrants further investigation to improve
632 model predictions.

633 Our results imply that the phytoplankton communities of the temperate microcosms initially
634 responded to the rapid increase in pCO_2 via a stress-induced response, resulting in large and

635 significant increases in DMS concentrations occurring over the shortest timescales (2 days),
636 with a lessening of the treatment effect with an increase in incubation time (Hopkins and
637 Archer 2014).

638 Within non-nutrient amended treatments such a reduction in response with time may also
639 have been driven by nutrient exhaustion, which could have lead the system to a similar state
640 across all CO_2 treatments, although we note that carbonate chemistry manipulation induced
641 responses were also similar within nutrient amended treatments (Richier et al. 2014, 2018).
642 The dominance of short response timescales in well-buffered temperate waters may also
643 indicate rapid acclimation of the phytoplankton populations following the initial stress
644 response, which forced the small-sized phytoplankton beyond their range of acclimative
645 tolerance and lead to increased DMS (Richier et al. 2018, Hopkins and Archer 2014).

646 This supports the hypothesis that populations from higher latitude, less well-buffered waters,
647 already possess a certain degree of acclimative tolerance to variations in carbonate chemistry
648 environment. Although initial community size structure was not a significant predictor of the
649 response to high CO_2, it is possible that a combination of both community composition and
650 the natural range in variability in carbonate chemistry – as a function of buffer capacity –
651 may influence the DMS/P response to OA over a range of timescales (Richier et al. 2018).

652 Our findings should be considered in the context of timescales of change (experimental vs
653 real world OA) and the potential of microbial communities to adapt to a gradually changing
654 environment. Microcosm experiments focus on the physiological response of microbial
655 communities to short term OA. Mesocosm experiments consider a timescale that allows the
656 response to be driven by community composition shifts, but are not long enough in duration
657 to incorporate an adaptive response. Neither approach is likely to accurately simulate the
658 response to the gradual changes in surface ocean pH that will occur over the next 50 – 100
659 years, nor the resulting changes in microbial community structure and distribution. However,
660 we hypothesise that the DMS response to OA should be considered not only in relation to
661 experimental perturbations to carbonate chemistry, but also in relation to the magnitude of
662 background variability in carbonate chemistry experienced by the DMS-producing organisms
663 and communities. Our findings suggest a strong link between the DMS response to OA and
664 background regional variability in the carbonate chemistry.

665 Models suggest the climate may be sensitive to changes in the spatial distribution of DMS
666 emissions over global scales (Woodhouse et al., 2013). Such changes could be driven by both

667 physiological and adaptive responses to environmental change. Accepting the limitations of
668 experimental approaches, our findings suggest that net DMS production from polar oceans
669 may be resilient to OA in the context of its short term effects on microbial communities. The
670 oceans face a multitude of CO_2-driven changes in the coming decades, including OA,
671 warming, deoxygenation and loss of sea ice (Gattuso et al., 2015). Our study addresses only
672 one aspect of these future ocean stressors, but contributes to our understanding of how DMS
673 emissions from the polar oceans may alter, facilitating a better understanding of Earth's
674 future climate.

675 ## Acknowledgements

676 This work was funded under the UK Ocean Acidification thematic programme (UKOA) via
677 the UK Natural Environment Research Council (NERC) grants to PD Nightingale and SD
678 Archer (NE/H017259/1) and to T Tyrell, EP Achterberg and CM Moore (NE/H017348/1).
679 The UK Department for Environment, Food and Rural Affairs (Defra) and the UK
680 Department of Energy and Climate Change (DECC) also contributed to funding UKOA. The
681 National Science Foundation, United States, provided additional support to SD Archer ((NSF
682 OCE-1316133). Our work and transit in the coastal waters of Greenland, Iceland and
683 Svalbard was granted thanks to permissions provided by the Danish, Icelandic and
684 Norwegian diplomatic authorities. We thank the captains and crew of the RRS Discovery
685 (cruise D366) and RRS James Clark Ross (cruises JR271 and JR274), and the technical staff
686 of the National Marine Facilities and the British Antarctic Survey. We are grateful to Mariana
687 Ribas-Ribas and Eithne Tynan for carbonate chemistry data, Elaine Mitchell and Clement
688 Georges for flow cytometry data, and Mariana Ribas-Ribas and Rob Thomas (BODC) for
689 data management.

690 ## References

691 Archer, S. D., Kimmance, S. A., Stephens, J. A., Hopkins, F. E., Bellerby, R. G. J., Schulz,
692 K. G., Piontek, J., and Engel, A.: Contrasting responses of DMS and DMSP to ocean
693 acidification in Arctic waters, Biogeosciences, 10, 1893-1908, doi: 10.5194/bg-10-1893-
694 2013, 2013.
695
696 Avgoustidi, V., Nightingale, P. D., Joint, I. R., Steinke, M., Turner, S. M., Hopkins, F. E.,
697 and Liss, P. S.: Decreased marine dimethyl sulfide production under elevated CO_2 levels in
698 mesocosm and in vitro studies, Environ. Chem., 9, 399-404, 2012.

Bigg, E. K., and Leck, C.: Properties of the aerosol over the central Arctic Ocean, J. Geophys. Res.-Atmos., 106, 32101-32109, 2001.

Brussaard, C. P. D., Noordeloos, A. A. M., Witte, H., Collenteur, M. C. J., Schulz, K., Ludwig, A., and Riebesell, U.: Arctic microbial community dynamics influenced by elevated CO_2 levels, Biogeosciences, 10, 719-731, doi: 10.5194/bg-10-719-2013, 2013.

Carpenter, L. J., Archer, S. D., and Beale, R.: Ocean-atmosphere trace gas exchange, Chem. Soc. Rev., 41, 6473-6506, 2012.

Chang, R. Y. W., Sjostedt, S. J., Pierce, J. R., Papakyriakou, T. N., Scarratt, M. G., Michaud, S., Levasseur, M., Leaitch, W. R., and Abbatt, J. P.: Relating atmospheric and oceanic DMS levels to particle nucleation events in the Canadian Arctic, J. Geophys. Res. – Atmos., 116, 2011.

Charlson, R. J., Lovelock, J. E., Andreae, M. O., and Warren, S. G.: Oceanic phytoplankton, atmospheric sulphur, cloud albedo and climate, Nature, 326, 655-661, 1987.

Chen, T., and Jang, M.: Secondary organic aerosol formation from photooxidation of a mixture of dimethyl sulfide and isoprene, Atmos. Environ., 46, 271-278, 2012.

Coello-Camba, A., Agustí, S., Holding, J., Arrieta, J. M., and Duarte, C. M.: Interactive effect of temperature and CO_2 increase in Arctic phytoplankton, Front. Mar. Sci., 1, 49, 2014.

Crawfurd, K. J., Alvarez-Fernandez, S., Mojica, K.D.A., Riebesell, U., and Brussaard, C. P. D.: Alterations in microbial community composition with increasing fCO_2: A mesocosm study in the eastern Baltic Sea, Biogeosciences, 14 (16), 3831 - 3849, 2017.

Davidson, A. T., McKinlay, J., Westwood, K., Thompson, P., van den Enden, R., de Salas, M., Wright, S., Johnson, R., and Berry, K.: Enhanced CO_2 concentrations change the structure of Antarctic marine microbial communities, Mar. Ecol. Prog. Ser., 552, 93 – 113, 2016.

733 Egleston, E. S., Sabine, C. L., and Morel, F. M. M.: Revelle revisited: Buffer factors that
734 quantify the response of ocean chemistry to changes in DIC and alkalinity, Global
735 Biogeochem. Cy., 24, doi:10.1029/2008gb003407, 2010.
736
737 Engel, A., Zondervan, I., Aerts, K., Beaufort, L., Benthien, A., Chou, L., Delille, B., Gattuso,
738 J.-P., Harlay, J., Heeman, C., Hoffman, L., Jacquet, S., Nejstgaard, J., Pizay, M.-D.,
739 Rochelle-Newall, E., Schneider, U., Terbrueggen, A., and Riebesell, U.: Testing the direct
740 effect of CO_2 concentrations on a bloom of the coccolithophorid *Emiliania huxleyi* in
741 mesocosm experiments, Limnol. Oceanogr., 50, 493-507, 2005.
742
743 Engel, A., Schulz, K., Riebesell, U., Bellerby, R., Delille, B., and Schartau, M.: Effects of
744 CO_2 on particle size distribution and phytoplankton abundance during a mesocosm bloom
745 experiment (PeECE II), Biogeosciences, 5, 509-521, 2008.
746
747 Eppley, R. W.: Temperature and phytoplankton growth in the sea, Fish. B. - NOAA, 70,
748 1063-1085, 1972.
749
750 Fassbender, A. J., Sabine, C. L., and Feifel, K. M.: Consideration of coastal carbonate
751 chemistry in understanding biological calcification, Geophys. Res. Lett., 43, 4467-4476,
752 doi:10.1002/2016gl068860, 2016.
753
754 Flynn, K. J., Blackford, J. C., Baird, M. E., Raven, J. A., Clark, D. R., Beardall, J., Brownlee,
755 C., Fabian, H., and Wheeler, G. L.: Changes in pH at the exterior surface of plankton with
756 ocean acidification, Nat. Clim. Change, 2, 510-513, 2012.
757
758 Gabric, A. J., Qu, B., Matrai, P. A., Murphy, C., Lu, H., Lin, D. R., Qian, F., and Zhao, M.:
759 Investigating the coupling between phytoplankton biomass, aerosol optical depth and sea-ice
760 cover in the Greenland Sea, Dynam. Atmos. Oceans, 66, 94-109, doi:
761 10.1016/j.dynatmoce.2014.03.001, 2014.
762
763 Gattuso, J.-P., Lee, K., Rost, B., and Schulz, K.: Approaches and tools to manipulate the
764 carbonate chemistry, in: Guide to Best Practices for Ocean Acidification Research and Data
765 Reporting, edited by: Riebesell, U., Fabry, V. J., Hansson, L., and Gattuso, J. P.,
766 Pulblications Office of the European Union, Luxembourg, 263, 2010.

Gattuso, J.-P., Magnan, A., Bille, R., Cheung, W., Howes, E., Joos, F., Allemand, D., Bopp, L., Cooley, S., and Eakin, C.: Contrasting futures for ocean and society from different anthropogenic CO_2 emissions scenarios, Science, 349, aac4722, 2015.

Hagens, M., and Middelburg, J. J.: Attributing seasonal pH variability in surface ocean waters to governing factors, Geophys. Res. Lett., 43, 12,528-512,537, doi:10.1002/2016GL071719, 2016.

Holding, J. M., Duarte, C. M., Sanz-Martin, M., Mesa, E., Arrieta, J. M., Chierici, M., Hendriks, I. E., Garcia-Corral, L. S., Regaudie-de-Gioux, A., Delgado, A., Reigstad, M., Wassmann, P., and Agusti, S.: Temperature dependence of CO_2-enhanced primary production in the European Arctic Ocean, Nat. Clim. Change, 5, 1079, doi: 10.1038/nclimate2768, 2015.

Hönisch, B., Ridgwell, A., Schmidt, D. N., Thomas, E., Gibbs, S. J., Sluijs, A., Zeebe, R., Kump, L., Martindale, R. C., Greene, S. E., Kiessling, W., Ries, J., Zachos, J. C., Royer, D. L., Barker, S., Marchitto, T. M., Moyer, R., Pelejero, C., Ziveri, P., Foster, G. L., and Williams, B.: The Geological Record of Ocean Acidification, Science, 335, 1058-1063, doi: 10.1126/science.1208277, 2012.

Hopkins, F. E., Turner, S. M., Nightingale, P. D., Steinke, M., Bakker, D., and Liss, P. S.: Ocean acidification and marine trace gas emissions, P. Natl. Acad. Sci. USA, 107, 760-765, 2010.

Hopkins, F. E., and Archer, S. D.: Consistent increase in dimethyl sulfide (DMS) in response to high CO2 in five shipboard bioassays from contrasting NW European waters, Biogeosciences, 11, 4925-4940, doi:10.5194/bg-11-4925-2014, 2014.

Hoppe, C. J., Schuback, N., Semeniuk, D. M., Maldonado, M. T., and Rost, B.: Functional Redundancy Facilitates Resilience of Subarctic Phytoplankton Assemblages toward Ocean Acidification and High Irradiance, Front. Mar. Sci., 4, 229, 2017.

800 Hoppe, C. J. M., Hassler, C. S., Payne, C. D., Tortell, P. D., Rost, B., and Trimborn, S.: Iron
801 Limitation Modulates Ocean Acidification Effects on Southern Ocean Phytoplankton
802 Communities, PLOS ONE, 8, e79890, doi:10.1371/journal.pone.0079890, 2013.
803
804 Hoppe, C. J. M., Wolf, K. K. E., Schuback, N., Tortell, P. D., and Rost, B.: Compensation of
805 ocean acidification effects in Arctic phytoplankton assemblages, Nat. Clim. Change, 8, 529-
806 533, doi:10.1038/s41558-018-0142-9, 2018.
807
808 Hussherr, R., Levasseur, M., Lizotte, M., Tremblay, J.-É., Mol, J., Helmuth, T., Gosselin, M.,
809 Starr, M., Miller, L. A., and Jarniková, T.: Impact of ocean acidification on Arctic
810 phytoplankton blooms and dimethyl sulfide concentration under simulated ice-free and
811 under-ice conditions, Biogeosciences, 14, 2407, 2017.
812
813 Jarníková, T., and Tortell, P. D.: Towards a revised climatology of summertime
814 dimethylsulfide concentrations and sea–air fluxes in the Southern Ocean, Environ. Chem., 13,
815 364-378, doi:10.1071/EN14272, 2016.
816
817 Johnson, M. T., and Bell, T. G.: Coupling between dimethylsulfide emissions and the ocean-
818 atmosphere exchange of ammonia, Environ. Chem., 5, 259-267, doi:10.1071/EN08030, 2008.
819
820 Kapsenberg, L., Kelley, A. L., Shaw, E. C., Martz, T. R., and Hofmann, G. E.: Near-shore
821 Antarctic pH variability has implications for the design of ocean acidification experiments,
822 Sci. Rep. - UK, 5, 9638, doi:10.1038/srep09638, 2015.
823
824 Kiene, R. P., and Slezak, D.: Low dissolved DMSP concentrations in seawater revealed by
825 small-volume gravity filtration and dialysis sampling Limnol. Oceanogr.-Meth., 4, 80-95,
826 2006.
827
828 Kim, J. M., Lee, K., Shin, K., Kang, J. H., Lee, H. W., Kim, M., Jang, P. G., and Jang, M. C.:
829 The effect of seawater CO_2 concentration on growth of a natural phytoplankton assemblage
830 in a controlled mesocosm experiment, Limnol. Oceanogr., 51, 1629-1636, 2006.
831
832 Kim, J. M., Lee, K., Yang, E. J., Shin, K., Noh, J. H., Park, K. T., Hyun, B., Jeong, H. J.,
833 Kim, J. H., Kim, K. Y., Kim, M., Kim, H. C., Jang, P. G., and Jang, M. C.: Enhanced

834 Production of Oceanic Dimethylsulfide Resulting from CO2-Induced Grazing Activity in a
835 High CO_2 World, Environ. Sci. Technol., 44, 8140-8143, doi: 10.1021/es102028k, 2010.
836
837 Korhonen, H., Carslaw, K. S., Spracklen, D. V., Mann, G. W., and Woodhouse, M. T.:
838 Influence of oceanic dimethyl sulfide emissions on cloud condensation nuclei concentrations
839 and seasonality over the remote Southern Hemisphere oceans: A global model study, J.
840 Geophys. Res.-Atmos., 113, 16, D1520410.1029/2007jd009718, 2008a.
841
842 Korhonen, H., Carslaw, K. S., Spracklen, D. V., Ridley, D. A., and Ström, J.: A global model
843 study of processes controlling aerosol size distributions in the Arctic spring and summer, J.
844 Geophys. Res., 113, D08211, 2008b.
845
846 Lana, A., Bell, T. G., Simó, R., Vallina, S. M., Ballabrera-Poy, J., Kettle, A. J., Dachs, J.,
847 Bopp, L., Saltzman, E. S., Stefels, J., Johnson, J. E., and Liss, P. S.: An updated climatology
848 of surface dimethlysulfide concentrations and emission fluxes in the global ocean, Global
849 Biogeochem. Cy., 25, GB1004, 2011.
850
851 Leaitch, W. R., Sharma, S., Huang, L., Toom-Sauntry, D., Chivulescu, A., Macdonald, A.
852 M., von Salzen, K., Pierce, J. R., Bertram, A. K., and Schroder, J. C.: Dimethyl sulfide
853 control of the clean summertime Arctic aerosol and cloud, Elementa: Science of the
854 Anthropocene, 1, 000017, 2013.
855
856 Levasseur, M.: Impact of Arctic meltdown on the microbial cycling of sulphur, Nat. Geosci.,
857 6, 691-700, 2013.
858
859 Lewis, E., and Wallace, D. W. R.: Program Developed for CO_2 System Calculations, Carbon
860 Dioxide Information Analysis Center, Oak Ridge National Laboratory, U.S. Department of
861 Energy, Oak Ridge, Tennessee., 1998.
862
863 McCoy, D. T., Burrows, S. M., Wood, R., Grosvenor, D. P., Elliott, S. M., Ma, P.-L., Rasch,
864 P. J., and Hartmann, D. L.: Natural aerosols explain seasonal and spatial patterns of Southern
865 Ocean cloud albedo, Science Advances, 1 (6), e1500157, doi:10.1126/sciadv.1500157, 2015.
866

McNeil, B. I., and Matear, R. J.: Southern Ocean acidification: A tipping point at 450-ppm atmospheric CO_2, P. Natl. Acad. Sci. USA, 105, 18860-18864, doi:10.1073/pnas.0806318105, 2008.

Monier, A., Findlay, H. S., Charvet, S., and Lovejoy, C.: Late winter under ice pelagic microbial communities in the high Arctic Ocean and the impact of short-term exposure to elevated CO_2 levels, Front. Microbiol., 5, 490, 2014.

Orr, J. C., Fabry, V. J., Aumont, O., Bopp, L., Doney, S. C., Feely, R. A., Gnanadesikan, A., Gruber, N., Ishida, A., and Joos, F.: Anthropogenic ocean acidification over the twenty-first century and its impact on calcifying organisms, Nature, 437, 681-686, 2005.

Park, K.-T., Lee, K., Shin, K., Yang, E. J., Hyun, B., Kim, J.-M., Noh, J. H., Kim, M., Kong, B., Choi, D. H., Choi, S.-J., Jang, P.-G., and Jeong, H. J.: Direct Linkage between Dimethyl Sulfide Production and Microzooplankton Grazing, Resulting from Prey Composition Change under High Partial Pressure of Carbon Dioxide Conditions, Environ. Sci. Technol., 48, 4750-4756, doi:10.1021/es403351h, 2014.

Poulton, A. J., Daniels, C. J., Esposito, M., Humphreys, M. P., Mitchell, E., Ribas-Ribas, M., Russell, B. C., Stinchcombe, M. C., Tynan, E., and Richier, S.: Production of dissolved organic carbon by Arctic plankton communities: Responses to elevated carbon dioxide and the availability of light and nutrients, Deep-Sea Res. II: Topical Studies in Oceanography, 127, 60-74, doi:10.1016/j.dsr2.2016.01.002, 2016.

Raven, J., Caldeira, K., Elderfield, H., Hoegh-Guldberg, O., Liss, P., Riebesell, U., Shepherd, J., Turley, C., and Watson, A.: Ocean acidification due to increasing atmospheric carbon dioxide, The Royal Society, Policy Document 12/05, London, 2005.

Rempillo, O., Seguin, A. M., Norman, A. L., Scarratt, M., Michaud, S., Chang, R., Sjostedt, S., Abbatt, J., Else, B., and Papakyriakou, T.: Dimethyl sulfide air-sea fluxes and biogenic sulfur as a source of new aerosols in the Arctic fall, J. Geophys. Res.-Atmos., 116, 2011.

Richier, S., Achterberg, E. P., Dumousseaud, C., Poulton, A. J., Suggett, D. J., Tyrrell, T., Zubkov, M. V., and Moore, C. M.: Phytoplankton responses and associated carbon cycling

during shipboard carbonate chemistry manipulation experiments conducted around Northwest European shelf seas, Biogeosciences, 11, 4733-4752, doi: 10.5194/bg-11-4733-2014, 2014.

Richier, S., Achterberg, E. P., Humphreys, M. P., Poulton, A. J., Suggett, D. J., Tyrrell, T., and Moore, C. M.: Geographical CO_2 sensitivity of phytoplankton correlates with ocean buffer capacity, Glob. Change Biol., doi:10.1111/gcb.14324, 2018.

Riebesell, U., Gattuso, J. P., Thingstad, T. F., and Middelburg, J. J.: Preface "Arctic ocean acidification: pelagic ecosystem and biogeochemical responses during a mesocosm study", Biogeosciences, 10, 5619-5626, 10.5194/bg-10-5619-2013, 2013.

Sabine, C. L., Feely, R. A., Gruber, N., Key, R. M., Lee, K., Bullister, J. L., Wanninkhof, R., Wong, C. S., Wallace, D. W. R., Tilbrook, B., Millero, F. J., Peng, T.-H., Kozyr, A., Ono, T., and Rios, A. F.: The oceanic sink for anthropogenic CO_2, Science, 305, 367-371, 2004.

Schoemann, V., Becquevort, S., Stefels, J., Rousseau, V., and Lancelot, C.: Phaeocystis blooms in the global ocean and their controlling mechanisms: a review, J. Sea Res., 53, 43-66, 2005.

Schulz, K. G., Riebesell, U., Bellerby, R. G. J., Biswas, H., Meyerhofer, M., Muller, M. N., Egge, J. K., Nejstgaard, J. C., Neill, C., Wohlers, J., and Zollner, E.: Build-up and decline of organic matter during PeECE III, Biogeosciences, 5, 707-718, 2008.

Schulz, K. G., Bellerby, R. G. J., Brussaard, C. P. D., Büdenbender, J., Czerny, J., Engel, A., Fischer, M., Koch-Klavsen, S., Krug, S. A., Lischka, S., Ludwig, A., Meyerhöfer, M., Nondal, G., Silyakova, A., Stuhr, A., and Riebesell, U.: Temporal biomass dynamics of an Arctic plankton bloom in response to increasing levels of atmospheric carbon dioxide, Biogeosciences, 10, 161-180, 10.5194/bg-10-161-2013, 2013.

Schwinger, J., Tjiputra, J., Goris, N., Six, K. D., Kirkevåg, A., Seland, Ø., Heinze, C., and Ilyina, T.: Amplification of global warming through pH-dependence of DMS-production simulated with a fully coupled Earth system model, Biogeosciences, 14, 3633-3648, 2017.

Sharma, S., Chan, E., Ishizawa, M., Toom-Sauntry, D., Gong, S., Li, S., Tarasick, D., Leaitch, W., Norman, A., and Quinn, P.: Influence of transport and ocean ice extent on biogenic aerosol sulfur in the Arctic atmosphere, J. Geophys. Res. – Atmos., 117, 2012.

Six, K. D., Kloster, S., Ilyina, T., Archer, S. D., Zhang, K., and Maier-Reimer, E.: Global warming amplified by reduced sulphur fluxes as a result of ocean acidification, Nat. Clim. Change, 3, 975, 2013.

Stefels, J.: Physiological aspects of the production and conversion of DMSP in marine algae and higher plants, J. Sea Res., 43, 183-197, 2000.

Steinacher, M., Joos, F., Frolicher, T. L., Plattner, G. K., and Doney, S. C.: Imminent ocean acidification in the Arctic projected with the NCAR global coupled carbon cycle-climate model, Biogeosciences, 6, 515-533, 2009.

Stillman, J. H., and Paganini, A. W.: Biochemical adaptation to ocean acidification, J. Exp. Biol., 218, 1946-1955, 10.1242/jeb.115584, 2015.

Sunda, W., Kieber, D. J., Kiene, R. P., and Huntsman, S.: An antioxidant function for DMSP and DMS in marine algae, Nature, 418, 317-320, 2002.

Thoisen, C., Riisgaard, K., Lundholm, N., Nielsen, T. G., and Hansen, P. J.: Effect of acidification on an Arctic phytoplankton community from Disko Bay, West Greenland, Mar. Ecol. Prog. Ser., 520, 21-34, 2015.

Thomson, P. G., Davidson, A. T., and Maher, L.: Increasing CO2 changes community composition of pico- and nano-sized protists and prokaryotes at a coastal Antarctic site, Mar. Ecol. Prog. Ser., 554, 51-69, 2016.

Tortell, P. D., Payne, C. D., Li, Y., Trimborn, S., Rost, B., Smith, W. O., Riesselman, C., Dunbar, R. B., Sedwick, P., and DiTullio, G. R.: CO_2 sensitivity of Southern Ocean phytoplankton, Geophys. Res. Lett., 35, 2008.

967 Trimborn, S., Brenneis, T., Hoppe, C. J. M., Laglera, L. M., Norman, L., Santos-Echeandía,
968 J., Völkner, C., Wolf-Gladrow, D., and Hassler, C. S.: Iron sources alter the response of
969 Southern Ocean phytoplankton to ocean acidification, Mar. Ecol. Prog. Ser., 578, 35-50,
970 2017.
971
972 Tynan, E., Clarke, J. S., Humphreys, M. P., Ribas-Ribas, M., Esposito, M., Rérolle, V. M. C.,
973 Schlosser, C., Thorpe, S. E., Tyrrell, T., and Achterberg, E. P.: Physical and biogeochemical
974 controls on the variability in surface pH and calcium carbonate saturation states in the
975 Atlantic sectors of the Arctic and Southern Oceans, Deep Sea Res. Part II: Topical Studies in
976 Oceanography, doi:10.1016/j.dsr2.2016.01.001, 2016.
977
978 Vogt, M., Steinke, M., Turner, S., Paulino, A., Meyerhöfer, M., Riebesell, U., LeQuéré, C.,
979 and Liss, P.: Dynamics of dimethylsulphoniopropionate and dimethylsulphide under different
980 CO_2 concentrations during a mesocosm experiment, Biogeosciences, 5, 407-419, 2008.
981 von Glasow, R., and Crutzen, P. J.: Model study of multiphase DMS oxidation with a focus
982 on halogens, Atmos. Chem. Phys., 4, 589-608, 2004.
983
984 Webb, A. L., Malin, G., Hopkins, F. E., Ho, K. L., Riebesell, U., Schulz, K. G., Larsen, A.,
985 and Liss, P. S.: Ocean acidification has different effects on the production of dimethylsulfide
986 and dimethylsulfoniopropionate measured in cultures of Emiliania huxleyi and a mesocosm
987 study: a comparison of laboratory monocultures and community interactions, Environ.
988 Chem., doi:10.1071/EN14268, 2015.
989
990 Webb, A. L., Leedham-Elvidge, E., Hughes, C., Hopkins, F. E., Malin, G., Bach, L. T.,
991 Schulz, K., Crawfurd, K., Brussaard, C. P. D., Stuhr, A., Riebesell, U., and Liss, P. S.: Effect
992 of ocean acidification and elevated fCO_2 on trace gas production by a Baltic Sea summer
993 phytoplankton community, Biogeosciences, 13(15), 4595 – 4613, doi: 10.5194/bg-13-4595-
994 2016, 2016.
995
996 Woodhouse, M. T., Mann, G. W., Carslaw, K. S., and Boucher, O.: Sensitivity of cloud
997 condensation nuclei to regional changes in dimethyl-sulphide emissions, Atmos. Chem.
998 Phys., 13, 2723-2733, 10.5194/acp-13-2723-2013, 2013.

999 Table 1. Summary of the station locations and characteristic of the water sampled for the 18 microcosm experiments performed in temperate,
1000 sub-polar and polar waters. All polar stations were sampled for JR271 and JR274, with the exception of NS and IB.

Cruise	Station ID	Location	Sampling location	Sampling date	Sampling depth (m)	SST (°C)	Salinity	Nitrate (uM)	Total Chl *a* ($\mu g\ L^{-1}$)	$chl_{>10\ \mu m} : chl_{total}$	pCO_2 (µatm) T_0	pH (total) T_0	Experimental timepoints T_1, T_2 (hours)	Reference
D366	E01	Mingulay Reef	56°47.688N 7°24.300W	8 June 2011	6	11.3	34.8	1.1	3.3	no data	334.9	8.1	48, 96	*Hopkins & Archer (2014)*
	E02	Irish Sea	52°28.237N 5°54.052W	14 June 2011	5	11.8	34.4	0.3	3.5	0.80 ± 0.03	329.3	8.1	48, 96	*Hopkins & Archer (2014)*
	E02b	Bay of Biscay	46°29.794N 7°12.355W	19 June 2011	5	14.5	35.6	0.9	1.8	no data	340.3	8.1	48	*This study*
	E03	Bay of Biscay	46°12.137N 7°13.253W	21 June 2011	10	15.3	35.8	0.6	0.8	0.43 ± 0.03	323.9	8.1	48, 96	*Hopkins & Archer (2014)*
	E04	Southern North Sea	52°59.661N 2°29.841E	26 June 2011	5	14.6	34.1	0.9	1.3	0.19 ± 0.02	399.8	8.0	48, 96	*Hopkins & Archer (2014)*
	E04b	Mid North Sea	57°45.729N 4°35.434E	29 June 2011	5	13.2	34.8	No data	0.5	0.14 ± 0.003	327.3	8.1	48	*This study*
	E05	Mid North Sea	56°30.293N 3°39.506E	2 July 2011	12	14.0	35.0	0.2	0.3	0.23 ± 0.01	360.2	8.1	48, 96	*Hopkins & Archer (2014)*
	E05b	Atlantic Ocean	59°40.721N 4°07.633E	3 July 2011	4	13.4	30.7	0.3	0.7	0.12 ± 0.01	310.7	8.1	48	*This study*
	E06	Atlantic Ocean	59°59.011N 2°30.896E	3 July 2011	4	12.5	34.9	0.4	1.1	0.14 ± 0.01	287.1	8.2	48	*This study*
JR271	NS	Mid North Sea	56°15.59N 2°37.59E	3 June 2012	15	10.8	35.1	0.04	0.3	0.52 ± 0.05	300.5	8.2	48, 96	*This study*
	IB	Iceland Basin	60°35.39N 18°51.23W	8 June 2012	7	10.7	35.2	5.0	1.8	0.27 ± 0.02	309.7	8.1	48, 96	*This study*
	GG-AO	Greenland Gyre	76°10.52 N 2°32.96 W	13 June 2012	5	1.7	34.9	9.3	1.0	0.34 ± 0.001	289.3	8.2	48, 96	*This study*
	GI-AO	Greenland ice edge	78°21.15 N 3°39.85 W	18 June 2012	5	-1.6	32.6	4.2	2.7	0.78 ± 0.03	304.7	8.1	48, 96	*This study*
	BS-AO	Barents Sea	72°53.49 N 26°00.09 W	24 June 2012	5	6.6	35.0	5.4	1.3	0.04 ± 0.01	304.3	8.1	48, 96	*This study*
JR274	DP-SO	Drake Passage	58°22.00 S 56°15.12 W	13 Jan 2013	8	1.9	33.2	22.0	2.4	1.00 ± 0.06	279.3	8.2	48, 96	*This study*
	WS-SO	Weddell Sea	60°58.55 S 48°05.19 W	18 Jan 2013	6	-1.4	33.6	24.9	0.6	0.67 ± 0.06	510.5	7.9	72, 144	*This study*
	SG-SO	South Georgia	52°41.36 S 36°37.28 W	25 Jan 2013	5	2.2	33.9	24.1	0.7	0.35 ± 0.04	342.6	8.1	72, 144	*This study*
	SS-SO	South Sandwich	58°05.13 S 25°55.55 W	1 Feb 2013	7	0.5	33.7	18.5	4.6	0.57 ± 0.02	272.6	8.2	96, 168	*This study*

Table 2. Mean (± SD) ratio of >10µm Chl *a* to total Chl *a* ($chl_{>10µm}$:chl_{total}) for polar microcosm sampling stations. * indicates significant difference from the response to ambient CO_2.

Station	Time	ambient	550 µatm	750 µatm	1000 µatm	2000 µatm
GG						
	48 h	0.3 ± 0.1	0.3 ± 0.03	0.4 ± 0.2	0.3 ± 0.1	N/A
	96 h	1.0 ± 0.02	0.9 ± 0.2	0.8 ± 0.1	0.7 ± 0.2	
GI						
	48 h	1.0 ± 0.1	1.0 ± 0.1	0.8 ± 0.1	1.0 ± 0.0	N/A
	96 h	1.0 ± 0.1	1.1 ± 0.1	0.8 ± 0.1	0.8 ± 0.1	
BS						
	48 h	0.02 ± 0.01	0.04 ± 0.01	0.03 ± 0.01	0.02 ± 0.01	N/A
	96 h	0.04 ± 0.01	0.05 ± 0.04	0.05 ± 0.04	0.04 ± 0.04	
DP						
	48 h	1.0 ± 0.3	N/A	1.0 ± 0.1	N/A	N/A
	96 h	0.9 ± 0.1		1.0 ± 0.1		
WS						
	72 h	0.6 ± 0.1	N/A	0.7 ± 0.1	N/A	N/A
	144 h	0.7 ± 0.1		0.7 ± 0.1		
SG						
	72 h	0.3 ± 0.02	N/A	0.4 ± 0.1	0.3 ± 0.1	0.4 ± 0.03
	144 h	0.5 ± 0.1		0.6 ± 0.04	0.5 ± 0.1	0.4 ± 0.03
SS						
	96 h	0.7 ± 0.04	N/A	1.5 ± 0.1*	0.7 ± 0.02	1.6 ± 0.1*
	168 h	0.9 ± 0.2		1.4 ± 0.02*	0.8 ± 0.004	1.4 ± 0.2*

Figure 1. Surface (<5 m) concentrations (nM) of DMS (A-C) and total DMSP (D-F) for cruises in the NW European shelf (D366) (A,D), the sub-Arctic and Arctic Ocean (JR271) (B,E) and the Southern Ocean (JR274) (C,F). Locations of sampling stations for microcosm experiments shown in letters/numbers. E01 – E05: see Hopkins & Archer 2014. NS = *North Sea*, IB = *Iceland Basin*, GI = *Greenland Ice-edge*, GG = *Greenland Gyre*, BS = *Barents Sea*, DP = *Drake Passage*, WS = *Weddell Sea*, SG = *South Georgia*, SS = *South Sandwich*.

Figure 2. Depth profiles for all 18 sampling stations showing A. Temperature (°C), B. Salinity, C. Irradiance (µE m^{-2} s^{-1}), D. phototrophic nanoflagellate abundance (cells mL^{-1}), E. total bacteria abundance (cells mL^{-1}), F. total Chl a (µg L^{-1}), G. [DMS] (nM), H. total [DMSP] (nM) and I. DMS/DMSPt from CTD casts at sampling stations for microcosm experiments in temperate (green), Arctic (red) and Southern Ocean (blue) waters. See Table 1 for station details. Data for irrandiance, phototrophic nanoflagellates and total bacteria were not collected for temperate stations.

Figure 3. DMS concentrations (nmol L^{-1}) during experimental microcosms performed in Arctic waters (A - C) and in Southern Ocean waters (D – G). Data shown is mean of triplicate incubations, and error bars show standard error on the mean. Locations of water collection for microcosms shown in Figure 1 C – F.

Figure 4. Total DMSP (solid lines) and particulate DMSP (dashed lines) concentrations (nmol L^{-1}) during experimental microcosms performed in Arctic waters (A - C) and in Southern Ocean waters (D – G). Data shown is mean of triplicate incubations, and error bars show standard error on the mean. Locations of water collection for microcosms shown in

Figure 1 C – F. Particulate DMSP concentrations were used in calculations of DMSP production rates (Figure 5).

Figure 5. De novo synthesis of DMSP (μDMSP, d^{-1}) (left column) and DMSP production rates (nmol L^{-1} d^{-1}) (right column) for Arctic Ocean stations *Greenland Gyre* (A,B), *Greenland Ice-edge* (C, D) and Southern Ocean stations *Drake Passage* (E, F), *Weddell Sea* (G, H) and *South Georg*ia (I, J). No data is available for *Barents Sea* (Arctic Ocean) or *South Sandwich* (Southern Ocean).

Figure 6. Relationship between the ratio of dissolved inorganic carbon C_T to total alkalinity (C_T/A_T) of the sampled water and the relative CO_2 treatment effect at ($[x]_{highCO2}/[x]_{ambientCO2}$) for concentrations of DMS at T_1 (A) and T_2 (B), and for total DMSP concentrations at T_1 (C) and T_2 (D) for all microcosm experiments performed in NW European waters, sub-Arctic and Arctic waters, and the Southern Ocean. Grey solid line (= 1) indicates no effect of elevated CO_2. C_T/A_T>0.91 = polar waters (indicated by red dashed line). T_1 = 48 h, except for WS and SG (72 h) and SS (96 h). For detailed analyses of the NW European shelf data, see Hopkins & Archer (2014).

Figure 7. Relationship between the ratio of dissolved inorganic carbon C_T to alkalinity (C_T/A_T) of the sampled water and the relative CO_2 treatment effect at ($[x]_{highCO2}/[x]_{ambientCO2}$) for de novo DMSP synthesis (μDMSp, d^{-1}) at T_1 (A) and T_2 (B), and DMSP production rate (nmol L^{-1} d^{-1}) at T_1 (C) and T_2 (D) for microcosm experiments performed in NW European waters, sub-Arctic and Arctic waters, and the Southern Ocean. Grey solid line (= 1) indicates no effect of elevated CO_2. C_T/A_T>0.91 = polar waters (indicated by red dashed line). T_1 = 48 h, T2 = 96 h, except for *Weddell Sea* and *South Georgia* (72 h, 144 h). For discussion of the NW European shelf data, see Hopkins & Archer (2014).

Figure 8. Relationship between the ratio of dissolved inorganic carbon (C_T) to total alkalinity (C_T/A_T) of the sampled water and the relative CO_2 treatment effect ($[x]_{highCO2}/[x]_{ambientCO2}$) for chlorophyll *a* concentrations at T_1 (A) and T_2 (B) and phototrophic nanoflagellate abundance at T1 (C) and T2 (D) for all microcosm experiments performed in NW European waters, sub-Arctic and Arctic waters, and the Southern Ocean. Grey solid line (= 1) indicates no effect of elevated CO_2. C_T/A_T>0.91 = polar waters (indicated by red dashed line). T_1 = 48 h, T_2 = 96 h, except for *Weddell Sea* and *South Georgia* (72 h, 144 h) and *South Sandwich* (96 h, 168 h).

Figure 9. Variation in underway surface ocean carbonate chemistry parameters across the NW European shelf, Arctic Ocean and Southern Ocean for each of the cruises in this study. A. Seawater pCO_2 (μatm), B. Seawater $[H^+]$ (M), C. dissolved inorganic carbon (C_T) to total alkalinity (A_T) ratio (C_T/A_T), D. Carbonate ion concentration (CO_3^{2-}) (μmol kg^{-1}), E. Calcite saturation state ($\Omega_{calcite}$), F. Aragonite saturation state ($\Omega_{aragonite}$).

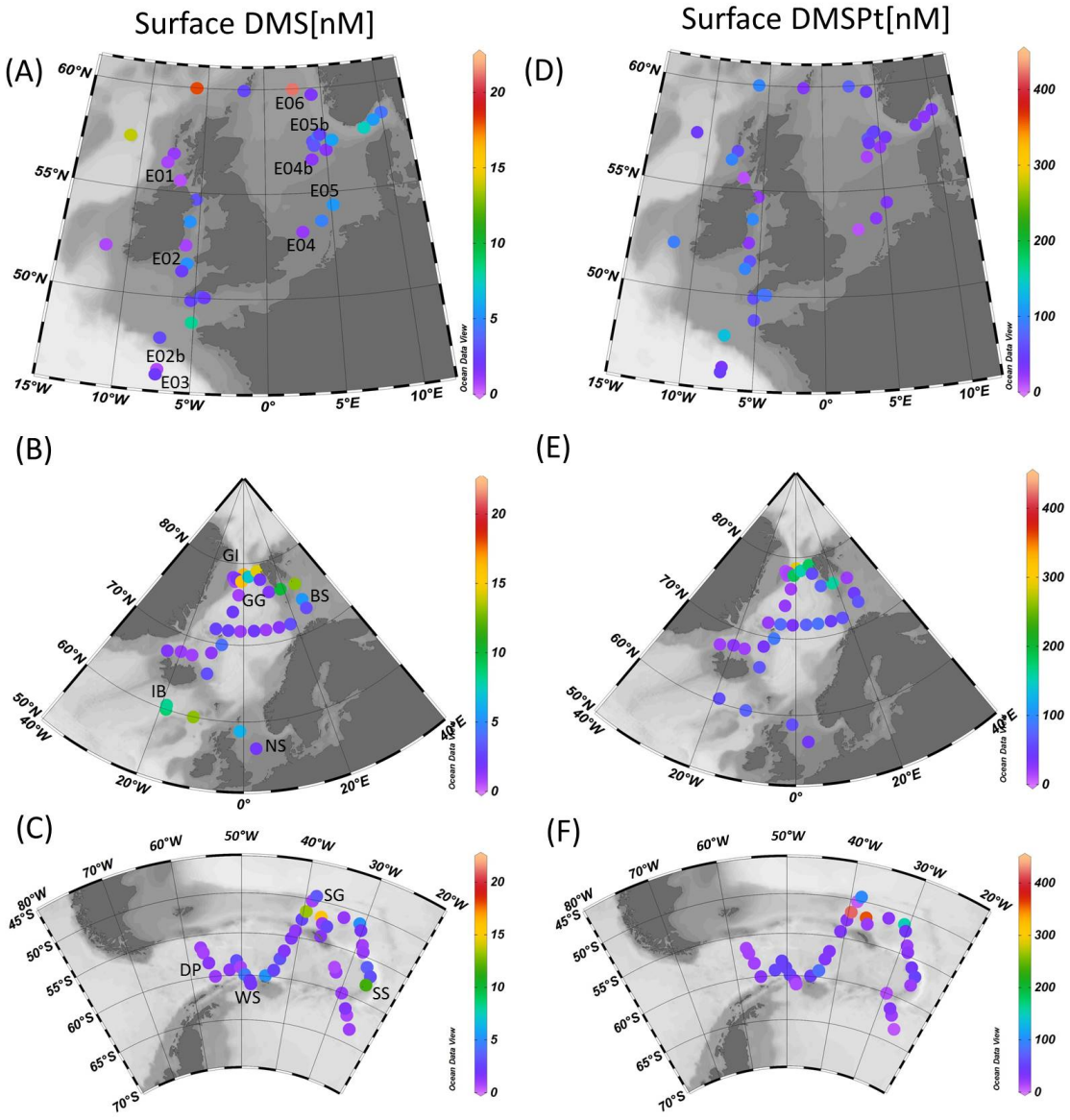

1062

1063

1064 Figure 1.

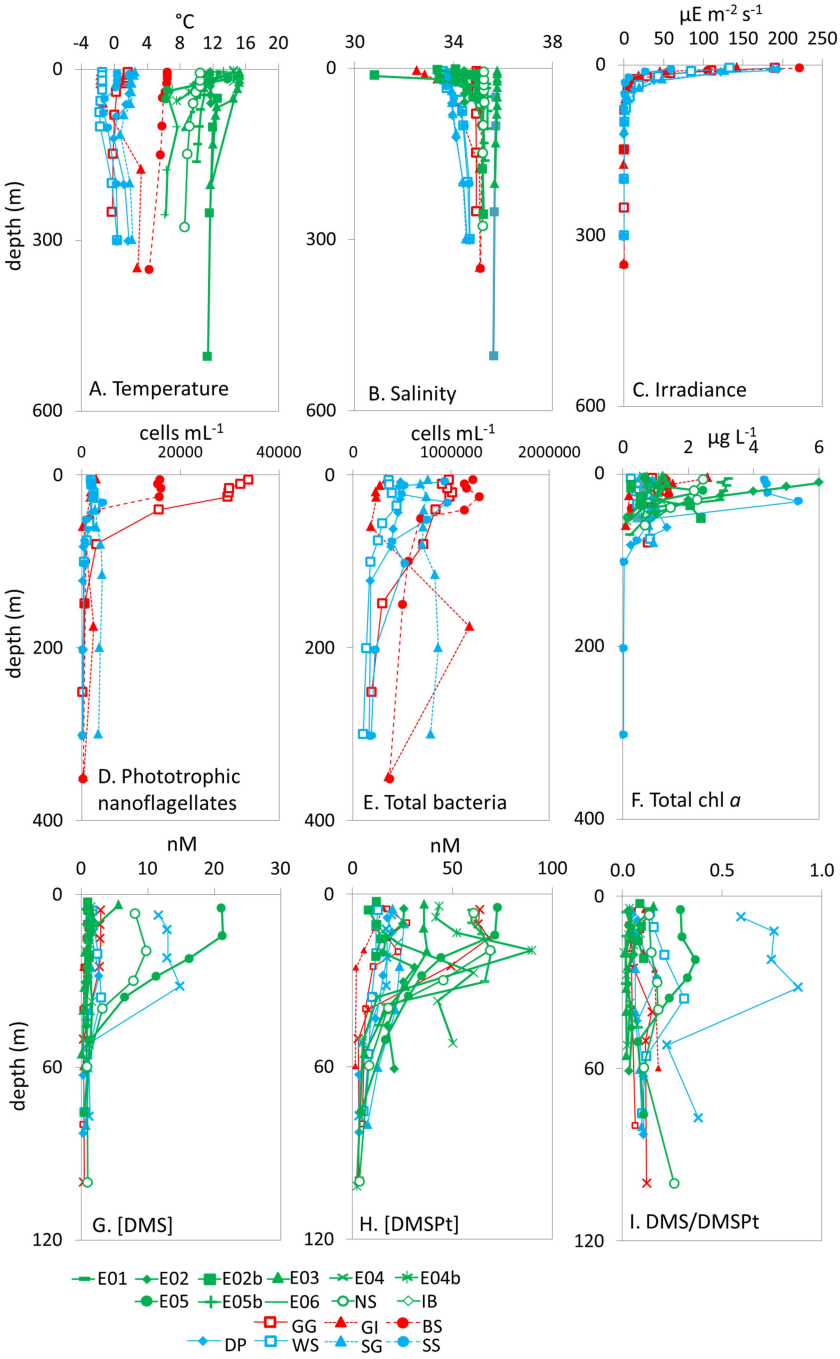

1065

1066 Figure 2.

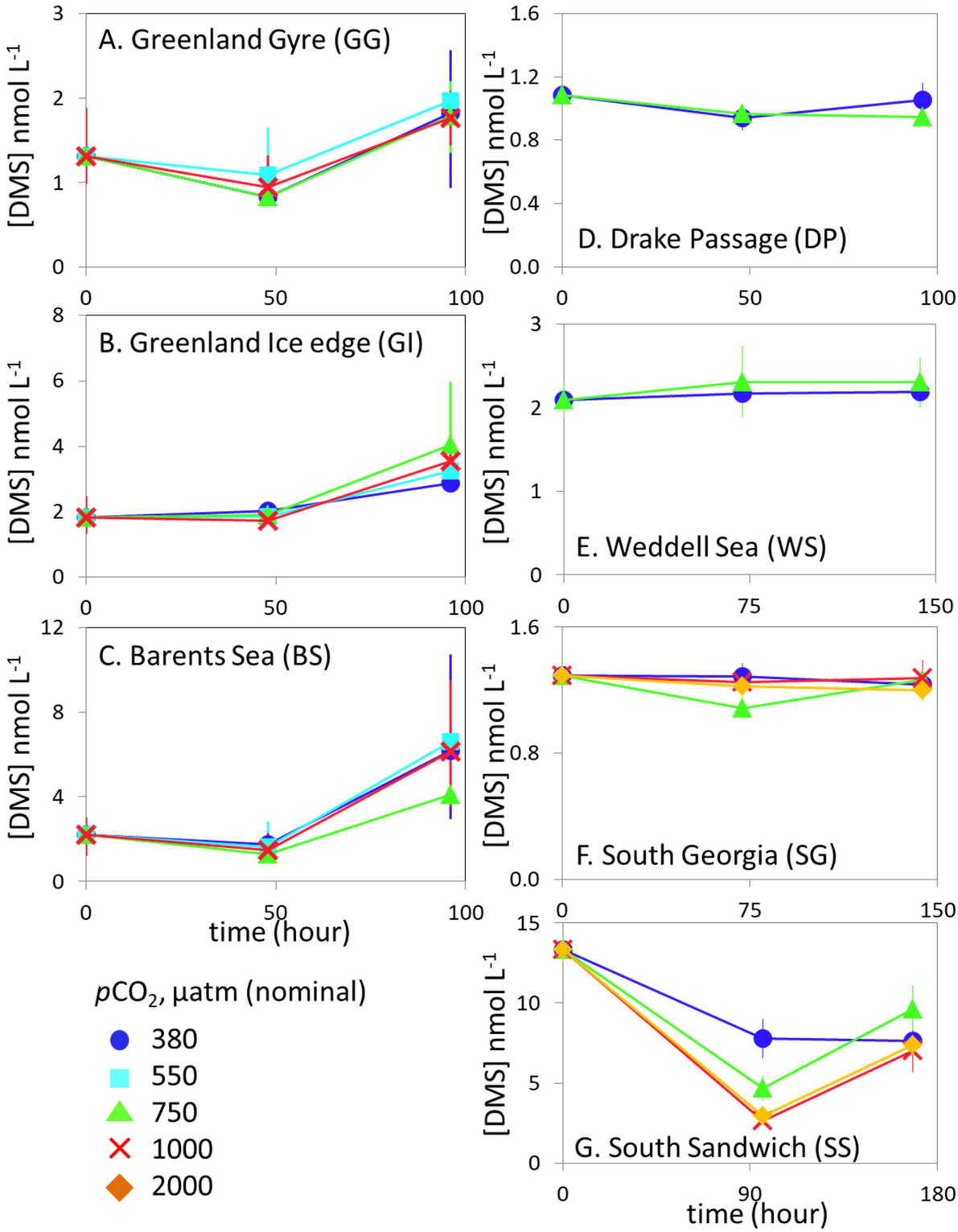

1067

1068 Figure 3.

1069

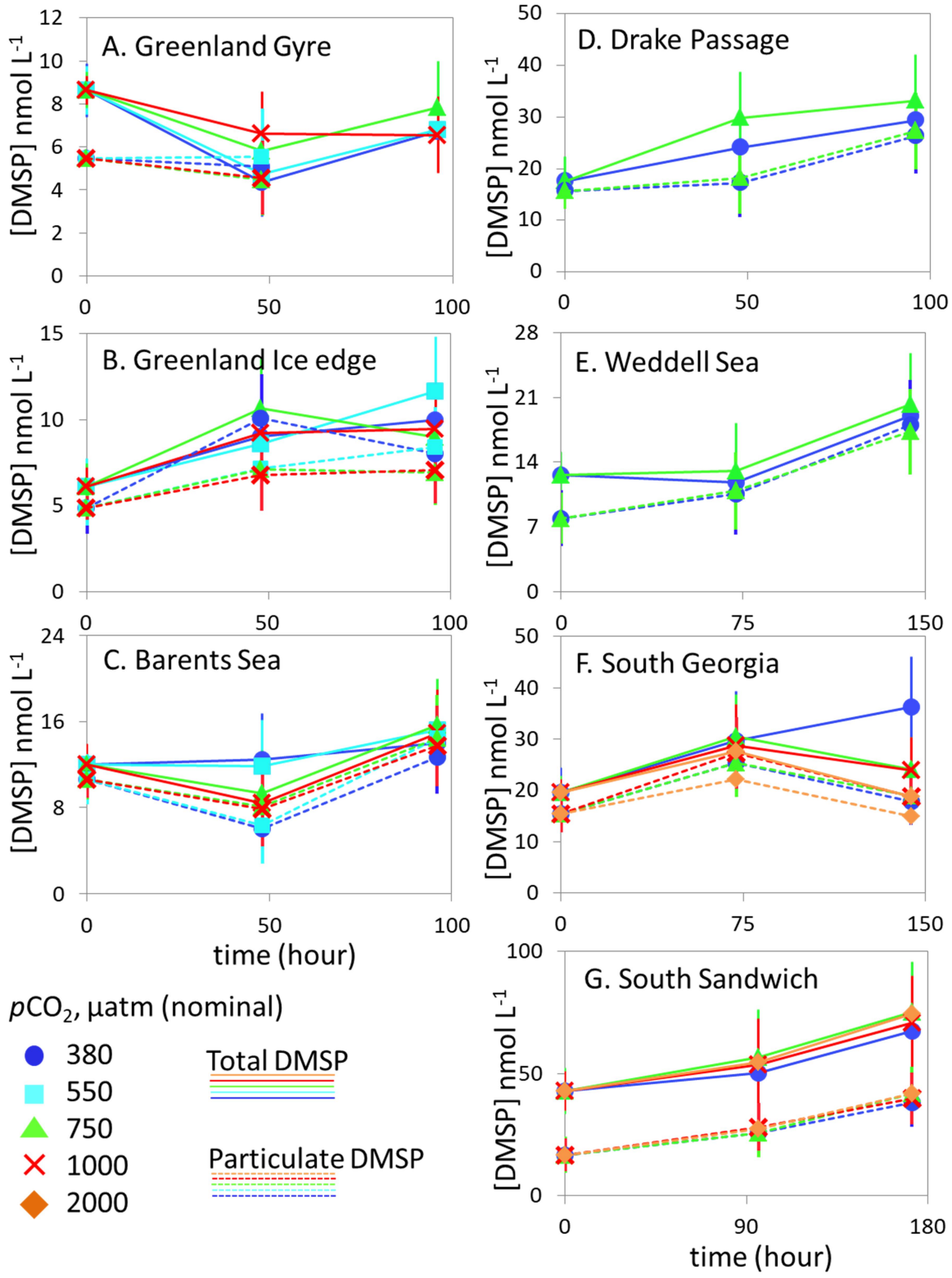

1070

1071 Figure 4.

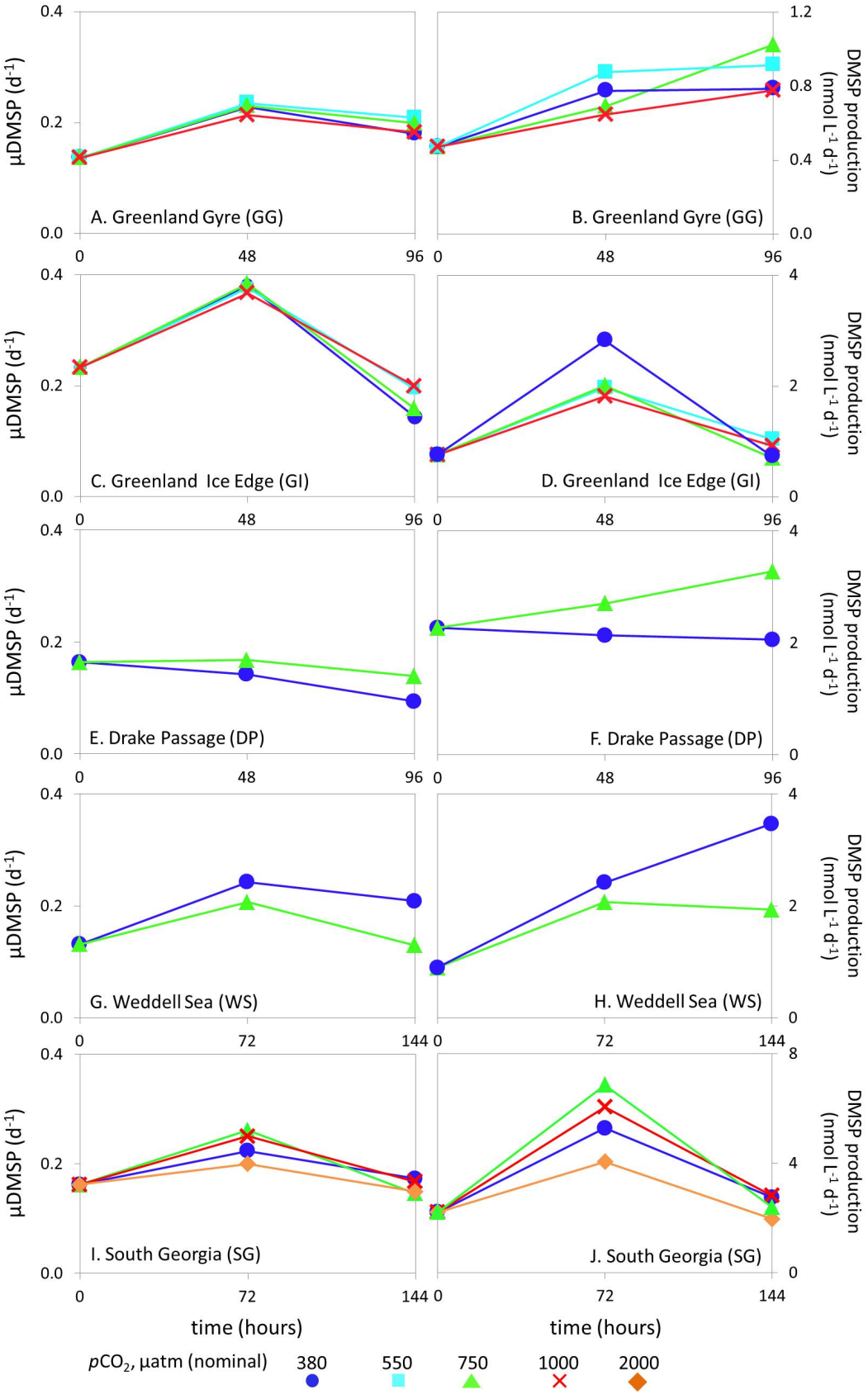
A. Greenland Gyre (GG)
B. Greenland Gyre (GG)
C. Greenland Ice Edge (GI)
D. Greenland Ice Edge (GI)
E. Drake Passage (DP)
F. Drake Passage (DP)
G. Weddell Sea (WS)
H. Weddell Sea (WS)
I. South Georgia (SG)
J. South Georgia (SG)
µDMSP (d-1)
DMSP production (nmol L-1 d-1)
time (hours)
pCO2, µatm (nominal)
380
550
750
1000
2000

Figure 5.

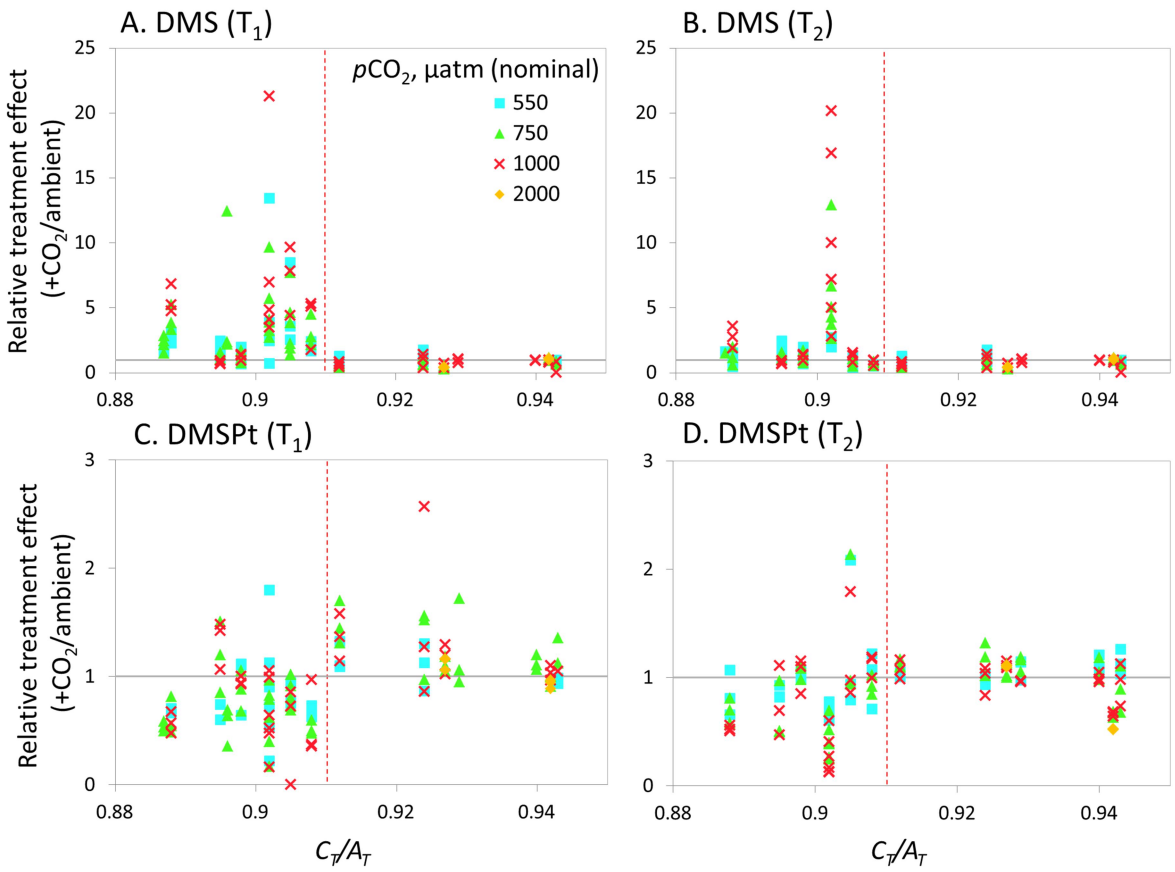

1075

1076 Figure 6.

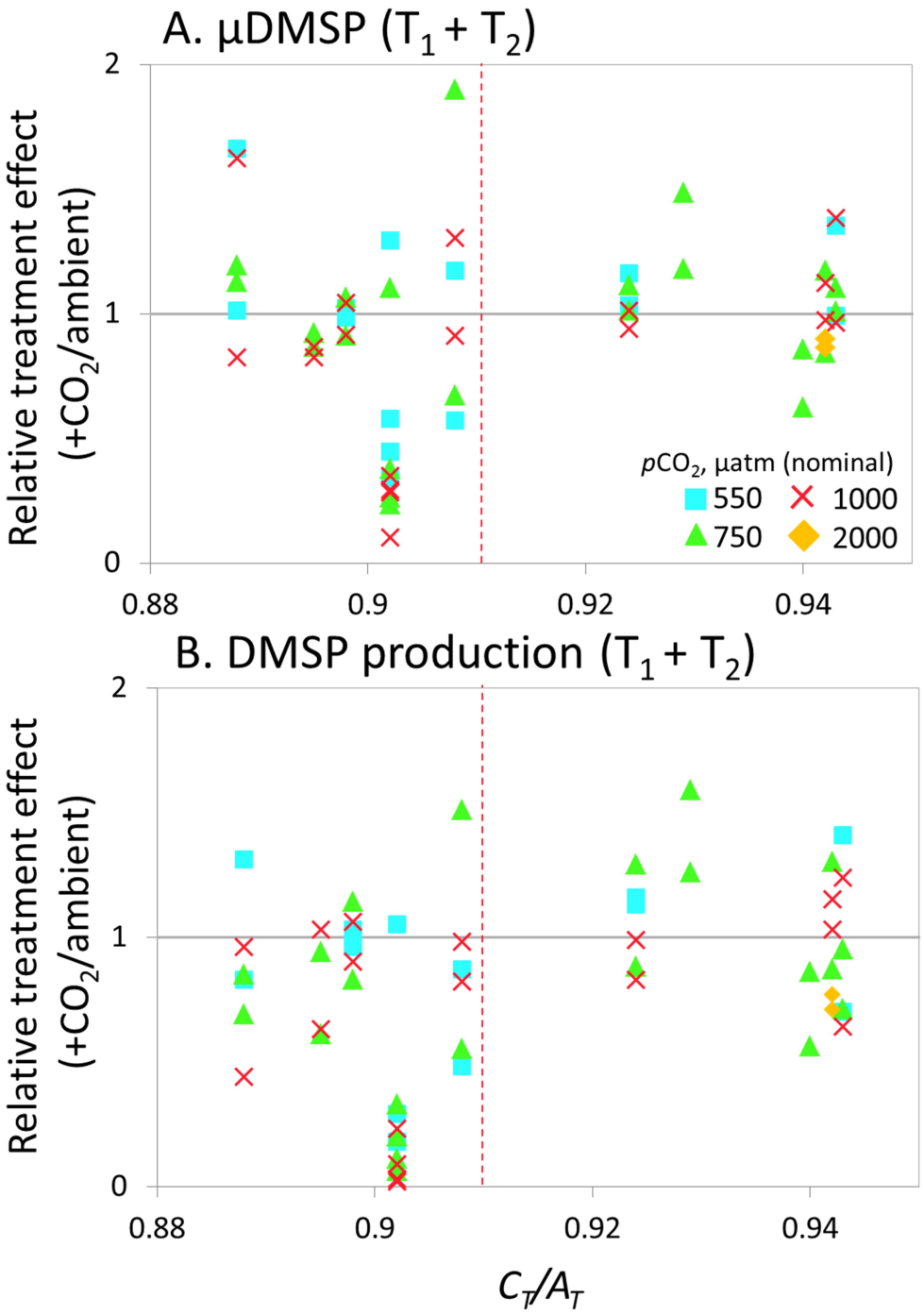

1077

1078 Figure 7.

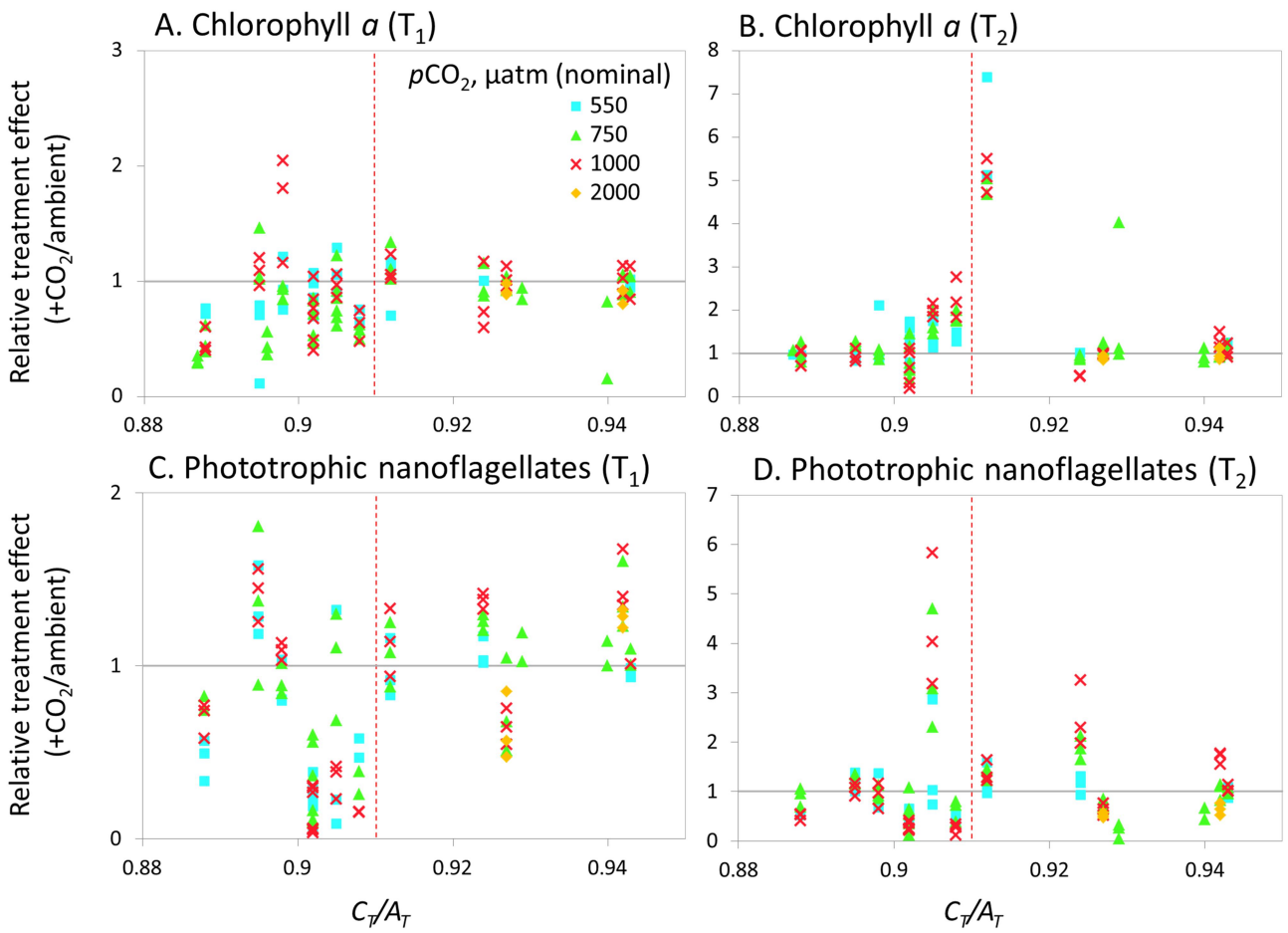
A. Chlorophyll a (T1)
B. Chlorophyll a (T2)
C. Phototrophic nanoflagellates (T1)
D. Phototrophic nanoflagellates (T2)
Relative treatment effect (+CO2/ambient)
pCO2, µatm (nominal)
550
750
1000
2000
CT/AT

Figure 8.

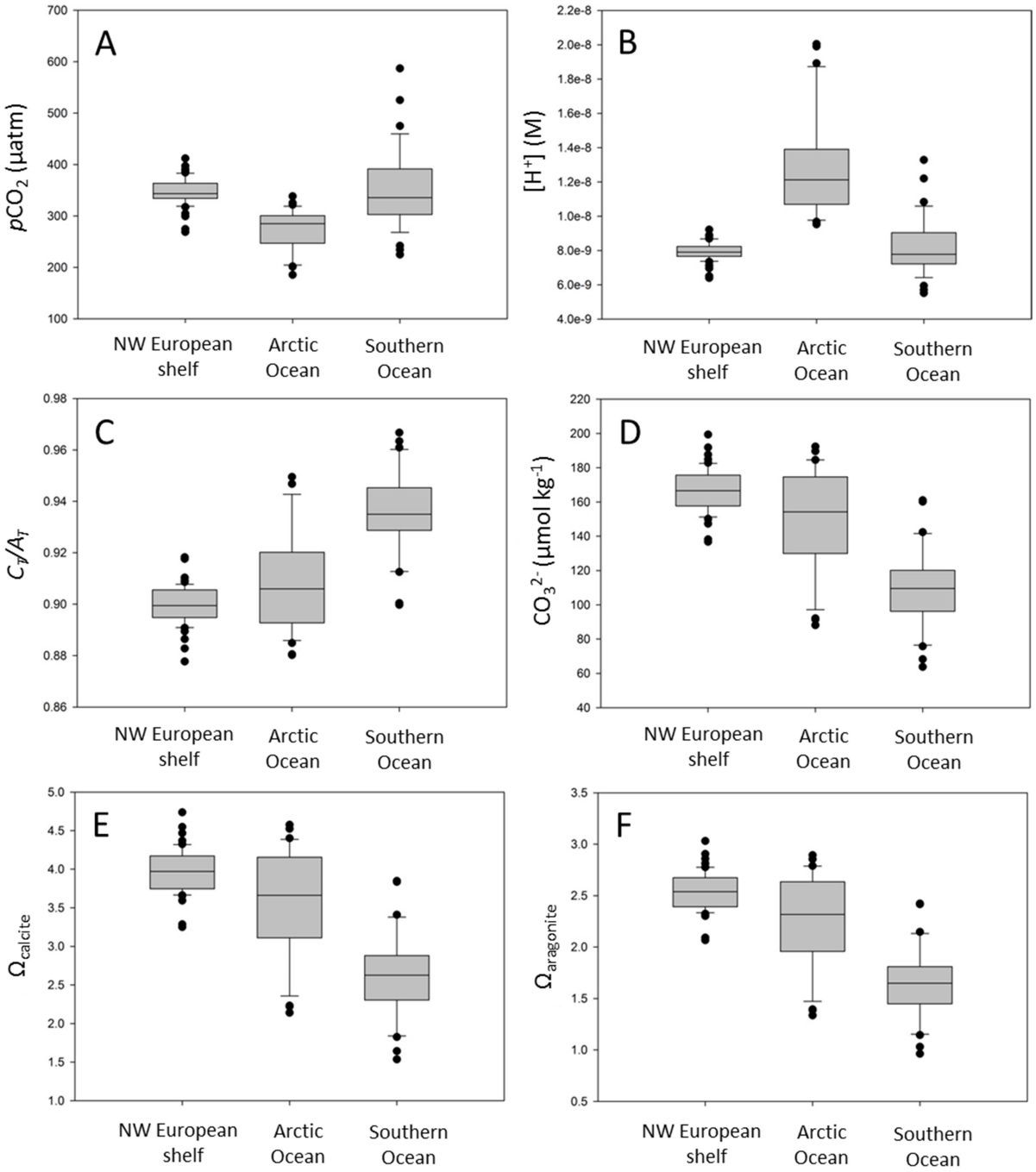

1081

1082 Figure 9.

1083

1084

1085